Inorganic Chemistry

Article

pubs.acs.org/IC

Multimetallic Complexes and Functionalized Gold Nanoparticles Based on a Combination of d- and f-Elements

Simon Sung,[†] Holly Holmes,[†] Luke Wainwright,[†] Anita Toscani,[†] Graeme J. Stasiuk,[†] Andrew J. P. White,[†] Jimmy D. Bell,[‡] and James D. E. T. Wilton-Ely*[,†]

[†]Department of Chemistry, Imperial College London, South Kensington Campus, London SW7 2AZ, United Kingdom

[‡]Metabolic and Molecular Imaging Group, MRC Clinical Sciences Centre, Imperial College London, Hammersmith Hospital, London W12 0NN, United Kingdom

Supporting Information

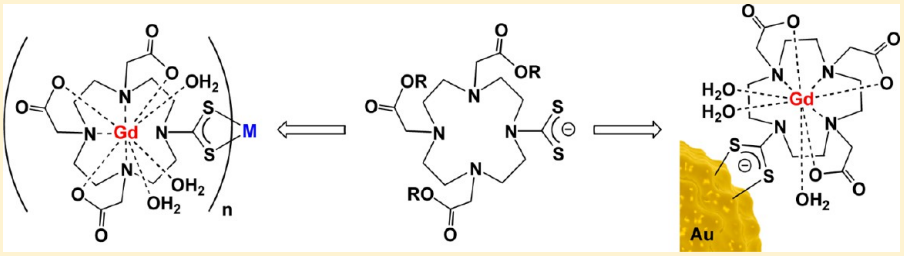

ABSTRACT: The new DO3A-derived dithiocarbamate ligand, DO3A-^{t}Bu-CS_2K, is formed by treatment of the ammonium salt [DO3A-^{t}Bu]HBr with K_2CO_3 and carbon disulfide. DO3A-^{t}Bu-CS_2K reacts with the ruthenium complexes *cis*-$[RuCl_2(dppm)_2]$ and $[Ru(CH{=}CHC_6H_4Me\text{-}4)Cl(CO)(BTD)(PPh_3)_2]$ (BTD = 2,1,3-benzothiadiazole) to yield $[Ru(S_2C\text{-}DO3A\text{-}^tBu)(dppm)_2]^+$ and $[Ru(CH{=}CHC_6H_4Me\text{-}4)(S_2C\text{-}DO3A\text{-}^tBu)(CO)(PPh_3)_2]$, respectively. Similarly, the group 10 metal complexes $[Pd(C,N\text{-}C_6H_4CH_2NMe_2)Cl]_2$ and $[PtCl_2(PPh_3)_2]$ form the dithiocarbamate compounds, $[Pd(C,N\text{-}C_6H_4CH_2NMe_2)(S_2C\text{-}DO3A\text{-}^tBu)]$ and $[Pt(S_2C\text{-}DO3A\text{-}^tBu)(PPh_3)_2]^+$, under the same conditions. The linear gold complexes $[Au(S_2C\text{-}DO3A\text{-}^tBu)(PR_3)]$ are formed by reaction of $[AuCl(PR_3)]$ (R = Ph, Cy) with DO3A-^{t}Bu-CS_2K. However, on reaction with [AuCl(tht)] (tht = tetrahydrothiophene), the homoleptic digold complex $[Au(S_2C\text{-}DO3A\text{-}^tBu)]_2$ is formed. Further homoleptic examples, $[M(S_2C\text{-}DO3A\text{-}^tBu)_2]$ (M = Ni, Cu) and $[Co(S_2C\text{-}DO3A\text{-}^tBu)_3]$, are formed from treatment of $NiCl_2{\cdot}6H_2O$, $Cu(OAc)_2$, or $Co(OAc)_2$, respectively, with DO3A-^{t}Bu-CS_2K. The molecular structure of $[Ni(S_2C\text{-}DO3A\text{-}^tBu)_2]$ was determined crystallographically. The *tert*-butyl ester protecting groups of $[M(S_2C\text{-}DO3A\text{-}^tBu)_2]$ (M = Ni, Cu) and $[Co(S_2C\text{-}DO3A\text{-}^tBu)_3]$ are cleaved by trifluoroacetic acid to afford the carboxylic acid products, $[M(S_2C\text{-}DO3A)_2]$ (M = Ni, Cu) and $[Co(S_2C\text{-}DO3A)_3]$. Complexation with Gd(III) salts yields trimetallic $[M(S_2C\text{-}DO3A\text{-}Gd)_2]$ (M = Ni, Cu) and tetrametallic $[Co(S_2C\text{-}DO3A\text{-}Gd)_3]$, with r^1 values of 11.5 (Co) and 11.0 (Cu) $mM^{-1}\ s^{-1}$ per Gd center. DO3A-^{t}Bu-CS_2K can also be used to prepare gold nanoparticles, Au@S_2C-DO3A-^{t}Bu, by displacement of the surface units from citrate-stabilized nanoparticles. This material can be transformed into the carboxylic acid derivative Au@S_2C-DO3A by treatment with trifluoroacetic acid. Complexation with $Gd(OTf)_3$ or $GdCl_3$ affords Au@S_2C-DO3A-Gd with an r^1 value of 4.7 $mM^{-1}\ s^{-1}$ per chelate and 1500 $mM^{-1}\ s^{-1}$ per object.

INTRODUCTION

Incorporating more than one metal unit into the same covalent framework leads to great potential benefits, especially if the properties of the different metals are complementary. Such multimetallic compounds are now finding application in areas as diverse as catalysis, imaging, therapy, and sensing.[1a]

While coordination polymers[1b,c] and metal−organic frameworks (MOFs)[2] are two of the most high-profile settings for assemblies containing many metals, the metals being connected are often the same. Linking two different metal centers has traditionally proved challenging, often requiring protection/deprotection strategies. Alternatively, the donor combinations of the connector can be chosen carefully to give selectivity for certain metals over others.[3a] Our recent contributions[3b−g] have explored dithiocarbamate-based linkers based on the zwitterion, $H_2NC_4H_8NCS_2$, which reacts with metals selectively at the dithiocarbamate unit. Subsequent deprotonation of the ammonium ion with base and treatment with carbon disulfide yields a new dithiocarbamate, allowing addition of a second, different metal unit. In addition to successfully providing a simple route to heteromultimetallic complexes (2−6 metal units), this approach has also been used to prepare nanoparticles functionalized with ruthenium and nickel transition metal units.[4]

The clear difference in donor affinity of late transition metals (soft) and lanthanide ions (hard) led us to explore the possibility of using dithiocarbamates as a means of preparing polylanthanide systems suitable for application in magnetic resonance imaging (MRI).

Received: July 26, 2013
Published: February 4, 2014

   dx.doi.org/10.1021/ic401936w | *Inorg. Chem.* 2014, 53, 1989−2005

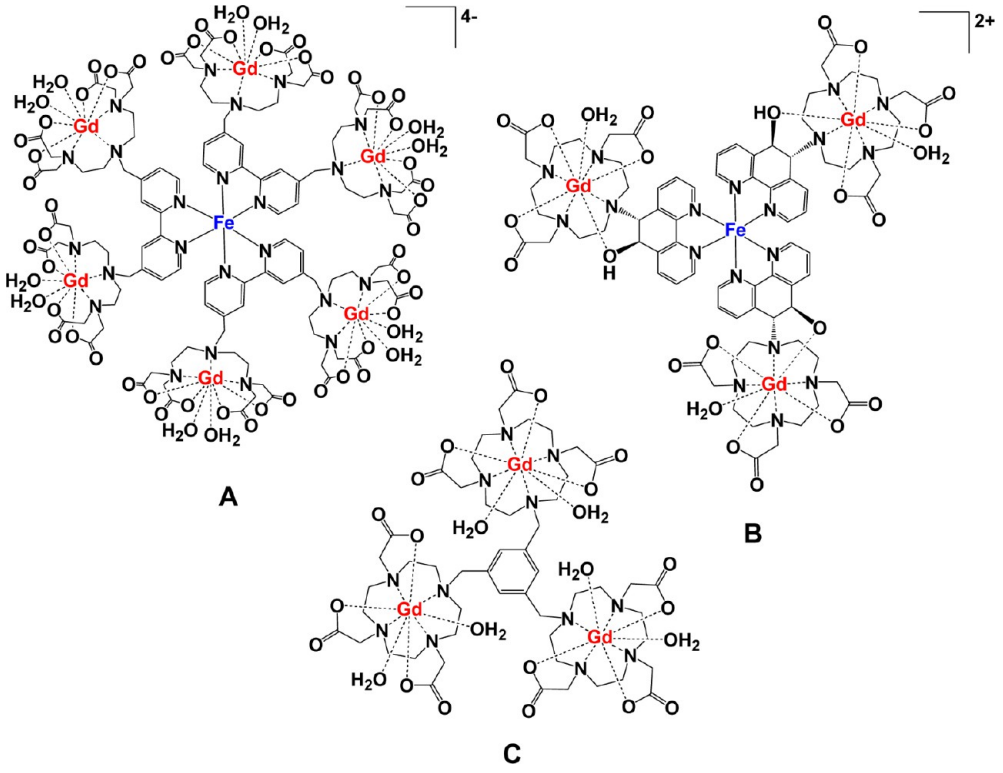

Figure 1. Multimetallic complexes designed for use in MRI.

MRI is a very important noninvasive medical imaging technique; however, the slow inate relaxation of water protons often requires the introduction of paramagnetic contrast agents to enhance the image quality. Among molecular contrast agents, gadolinium(III) is the dominant ion employed to achieve this, owing to its very slow electronic-spin relaxation rate, seven unpaired 4f electrons, and biological stability upon chelation by high denticity ligands.[5,6] The coordination of Gd(III) ions must provide both kinetic and thermodynamic stability *in vivo* to prevent transmetalation of the toxic ion by other endogenous metals, spontaneous dissociation, and transligation.[7,8]

Clinically used contrast agents are currently administered in high concentrations (0.1 mmol/kg) in order for their effects to be significant.[9] As a result, development of new compounds with high relaxivity is important to improve the sensitivity of MRI, which in turn should lead to better image quality, allow the use of lower doses, and thus reduce the risks of Gd(III) associated cytotoxicity. In addition to low toxicity, successful MRI contrast agents must possess other attributes, many of which depend on the number (hydration number, q) and residence lifetime (τ_M) of water molecules at the Gd(III) center. Another important factor that can have a large effect on the relaxivity is the rotational correlation time (τ_R) of the Gd(III) complex.[9] Increasing the rotational correlation time leads to an increased relaxation rate; therefore, increasing the size of the contrast agents is an attractive method to improve performance.[10] Having a highly symmetric contrast agent with rigid bonds is also advantageous because the rotational dynamics are more isotropic, which enhances the effect of the large molecular mass on improving relaxivity.[11]

Approaches to enhance the sensitivity of magnetic resonance contrast agents often focus on "increasing the payload", i.e., by delivering multiple Gd(III) chelates. The greater mass also increases τ_R and thus increases the relaxivity of the agent by slowing rotation. Multiple Gd(III) ions have been incorporated into single macromolecular species such as dendrimers[12] and linear polymers,[13,14] but these systems do not exhibit relaxivities as high as expected. In the linear polymer systems, the limited relaxivity was attributed to anisotropic rotational dynamics where the rotation about the short axis was fast. Dendrimeric polymer systems demonstrate higher relaxivities due to their more isotropic rotational dynamic.[9] However, the flexible linkages between the Gd(III) chelates and the dendrimer core allow movement of the chelates to be partially independent from the whole structure, which consequently limits the relaxivity.[12a] To counteract this undesired effect, multiple Gd(III) ions have been incorporated into metal templated self-assembled complexes containing traditional gadolinium-binding ligands such as DOTA (1,4,7,10-tetraaza-cyclododecane-1,4,7,10-tetraacetic acid) or DTPA (diethylene-triaminepentaacetic acid).[15] These systems are noted for their compact size (with respect to dendrimeric polymers), rigidity, and high number of Gd(III) ions. In cell imaging, having several Gd(III) ions in a small region of space can be an advantage over large macromolecules containing only a few Gd(III) ions, as a cell can only permit entry to a limited number of contrast agent molecules before they become highly cytotoxic and lead to cell death.[16]

The metallostar system of Tóth and co-workers (Figure 1, structure **A**) was found to be particularly impressive as its relaxivity of 33.2 mM^{-1} s^{-1} (60 MHz, 25 °C)[16] was comparable to that of a PAMAM [poly(amidoamine)] dendrimer system functionalized with Gd(DOTA) units (1860 Gd(III) ions), of much greater mass.[17] In addition, the high charge on the compound was found to aid water solubility. However, long-term studies conducted in mouse serum showed cleavage of the iron-bipyridine bonds, and in phosphate-buffered saline (PBS),

dx.doi.org/10.1021/ic401936w | *Inorg. Chem.* 2014, 53, 1989−2005

the inner-sphere water molecules were displaced by phosphate ions.[16b,18] Replacement of the iron(II) metal center with a more kinetically inert ruthenium(II) ion showed that the relaxation characteristics remained unchanged; however, *in vitro* and *in vivo* stability studies have not yet been reported.[19,20] While the $Fe(bpy)_3$ core of **A** was assumed to be essentially rigid, the local movement of the Gd(III) chelates was found to be 5 times faster than the motion of the entire molecule.[16b] The source of this flexibility within the assembly was traced to rotation about the methylene spacer between the Gd(III) chelates and the 2,2′-bipyridine groups. This aspect has been addressed in the phenanthroline-DO3A framework (**B**), shown in Figure 1, by reducing rotation through chelation of hydroxy units attached to the phenanthroline moiety.[21]

Multigadolinium(III) contrast agents have also been formed with the chelates linked without the use of d-block metals;[22,23] however, these compounds fail to exhibit relaxivities comparable to the metallostars of Tóth et al. For example, the lower relaxivity of the recently reported trigadolinium DO3A compound based on a mesitylene core, $Mes(DO3A\text{-}Gd)_3$ (Figure 1, structure **C**), was probably due to the anisotropic rotational character of the molecule and the flexibility permitted by the methylene group linkers.[24]

These examples illustrate the importance of combating the independent rotational flexibility of the peripheral Gd(III) units as well as the additional design required to achieve this. This factor was significant in the choice of the dithiocarbamate unit to link the metals in the multimetallic systems reported in this article. In both dithiocarbamate complexes and the ligand itself, the C−N bond typically shows substantial double bond character, which is attributed to the thioureide resonance form. This renders the nitrogen lone pair essentially unreactive toward other species,[25] and also leads to planarity of the R_2NCS_2M unit in complexes where bidentate coordination is present. As a result, the dithiocarbamate linkage between the transition metal center and the Gd(III) chelate should display minimal rotational flexibility.[25] However, this is a disadvantage in that the lack of interaction of the nitrogen with the Gd(III) center may leave this ion more susceptible to ligation by endogenous anions such as phosphates and bicarbonates.[26]

Another approach to the aim of bringing many Gd(III) centers into the same assembly has focused on the functionalization of the surface of gold nanoparticles with paramagnetic units.[27] This provides a complementary nanoparticle methodology to the use of superparamagnetic iron oxide (SPIO) nanoparticle contrast agents as Gd(III)-based agents shorten the longitudinal relaxation time (T_1) while SPIOs shorten the transverse relaxation time (T_2).[28] Recent developments in molecular and cellular imaging to detect disease specific molecular markers and interactions *in vivo* has led to increased interest in nanoparticles as a flexible platform.[29−39] As a result of recent advances in this field, new nanoparticulate MRI contrast agents have been developed, which enhance their imaging power by incorporating extra functionalities.[33]

The small size and large surface area of nanoparticles present many properties that can be utilized in MRI contrast agents. They exhibit reduced tumbling rates which, combined with their ability to carry high payloads of active magnetic centers, provide an enhancement of the relaxivity. Additionally, they have been shown to be biologically compatible and can penetrate biological membranes, though this is dependent on size. Larger nanoparticles can lead to prolonged circulation but also lead to clearance issues in the kidneys. Conjugation to affinity ligands (e.g., peptides or antibodies) allows them to be targeted at cells and then penetrate the cell membrane, depending on the groups attached. While further refinement is still needed, nanoparticulate MRI contrast agents offer the potential for the delivery of imaging with enhanced sensitivity and specificity at a low imaging agent concentration.

The pioneering work of Roux et al.[34,35] provides useful illustrations of some of the challenges associated with the attachment of Gd(III) units to the surface of gold nanoparticles. Modification of the diethylenetriaminepentaacetic acid (DTPA) chelate used in clinical contrast agents to include two thiol moieties (DTDPA) was anticipated to result in secure, two-site anchoring of the ligand to the nanoparticle surface. However, rather than both thiol units attaching to the gold, it was found that only one of the sulfur tethers was attached to the gold surface with the ungrafted thiols forming disulfide bonds between neighboring DTDPA units. As a result, the Au@DTDPA nanoparticles were synthesized with a multilayered shell of DTDPA. These nanoparticles (containing 150 gadolinium units) showed a moderate improvement in relaxivity (r^1 = 586 mM^{-1} s^{-1}) compared to the commercially available contrast agent, DTPA:Gd (r^1 = 3 mM^{-1} s^{-1}).[20] However, agglomeration of the nanoparticles occurred within 24 h, hampering their use *in vivo*. This behavior was attributed to the large number of Gd(III) ions incorporated per particle, which overcame the electrostatic repulsion required to maintain colloidal stability. This issue was resolved by reducing the number of Gd(III) ions from 150 to 50 per particle.[34] Subsequent strategies involved gold nanoparticles functionalized through a Gd-DTPA-bis(amide) conjugate of glutathione; however, the formation of disulfide bridges was again observed.[36]

The attachment of surface units in addition to the imaging modality is a major advantage of gold nanoparticles. This is exemplified in the work of Penadés and co-workers, who showed that the relaxivity of contrast agents could be tuned through the choice of sugar used as surface counit.[37] Furthermore, this potential for combining functional properties in these nanomaterials makes it possible to bring together multiple imaging modalities with the delivery of therapeutic agents.[40] For example, this approach has been employed to combine MR imaging and dark-field scattering microscopy to image cancer cells before selectively destroying them photothermally using NIR light.[41]

While significant developments have been achieved in the design of nanoparticle-based MR imaging agents, a number of issues have been unearthed with the use of thiols, such as the tendency to form disulfide linkages rather than interacting with the gold surface.[34,36] The thiol attachment strategies which employ a single thiol tether[29,37,38] are susceptible to the loss of the surface unit, especially under biological conditions, as observed commonly for many thiol-coated gold nanoparticles.[42] Furthermore, the introduction of thiols into the gadolinium chelate can often be synthetically challenging and result in a significant number of extra synthetic steps. The use of a dithiocarbamate, which can be readily prepared from a secondary amine and carbon disulfide, represents a straightforward approach. Additionally, it has been observed in the literature addressing dithiocarbamate functionalized gold nanoparticles that these surface units are more resistant to displacement than thiols.[43,44]

dx.doi.org/10.1021/ic401936w | *Inorg. Chem.* 2014, 53, 1989−2005

Scheme 1. Synthesis of the Dithiocarbamate Ligand (1)

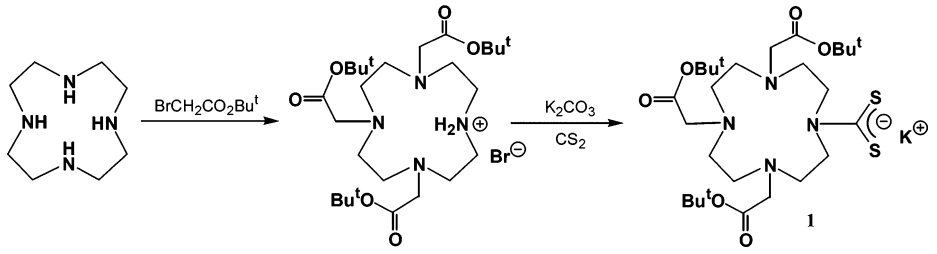

Scheme 2. Formation of Mononuclear Dithiocarbamate Complexes[a]

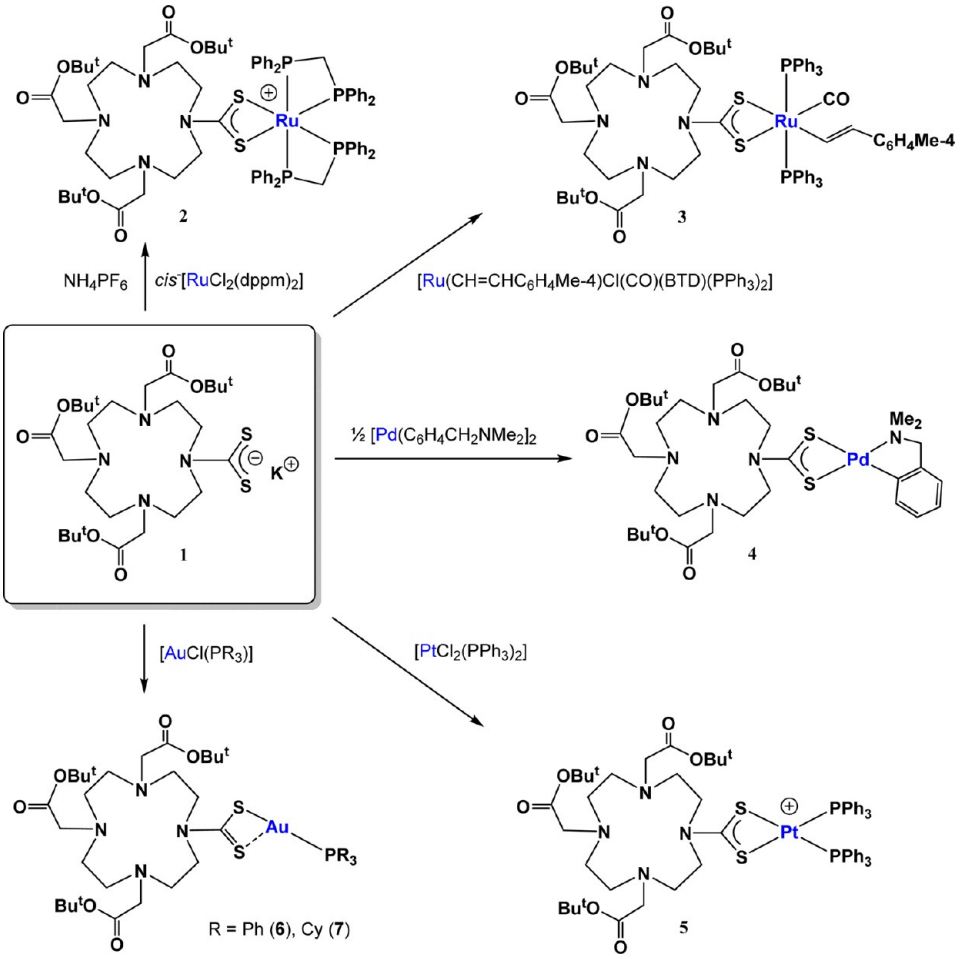

[a]BTD = 2,1,3-benzothiadiazole.

This article demonstrates how dithiocarbamate ligands based on the successful DO3A chelate[45] could be used in the development of assemblies suitable for magnetic resonance imaging applications. Initially, simple monometallic systems are used in order to establish the coordination chemistry before the synthesis of heterotri- and tetrametallic complexes. In parallel, the use of the same dithiocarbamate unit is explored in the functionalization of gold nanoparticles with paramagnetic Gd(III) centers.

RESULTS AND DISCUSSION

Synthesis of the Dithiocarbamate-Based Polydentate Chelate. Using a literature route,[46] cyclen was converted to the triester ammonium salt in good yield and in sufficient purity (^{1}H NMR analysis) that further purification was not required (Scheme 1). Various bases (NEt_3, DBU) were employed to deprotonate this compound, but potassium carbonate was found to work most efficiently in acetonitrile to yield the desired yellow dithiocarbamate (**1**) in 91% yield. Compound **1** was found to be soluble in most solvents apart from hydrocarbons (e.g., hexane). The infrared spectrum displayed absorptions assigned to the ester groups at 1721 ($\nu_{C=O}$) and 1151 cm^{-1} (ν_{C-O}), as well as ν_{C-N} and two ν_{C-S} bands attributed to the dithiocarbamate moiety at 1453 and 990 and 969 cm^{-1}, respectively. ^{1}H NMR analysis of **1** revealed resonances for the CH_2 protons in three separate multiplets between 2.33 and 6.40 ppm, while two singlets were observed for the distinct methyl environments at 1.45 and 1.47 ppm. The ^{13}C NMR spectrum showed resonances at typical chemical shift values for the substituted macrocyle, including a diagnostic

dx.doi.org/10.1021/ic401936w | Inorg. Chem. 2014, 53, 1989−2005

resonance for the CS_2 carbon at the characteristic low-field chemical shift of 224.3 ppm. Characterization of DO3A-^{t}Bu-CS_2K (**1**) was completed using mass spectrometry and elemental analysis.

Monometallic Complexes. In order to assess the coordination chemistry of the new dithiocarbamate ligand (**1**), a series of monometallic complexes was prepared displaying octahedral, square planar, and linear geometries. The Ru(II) complexes *cis*-$[RuCl_2(dppm)_2]$ and $[Ru(CH{=}CHC_6H_4Me\text{-}4)Cl(BTD)(CO)(PPh_3)_2]$ (BTD = 2,1,3-benzothiadiazole) were chosen as suitable reaction partners for **1** as they are known to react rapidly with a wide range of dithiocarbamate salts to give cationic and neutral species, respectively.[3f,4] The chloride ligands in *cis*-$[RuCl_2(dppm)_2]$ were displaced by **1** in the presence of NH_4PF_6 to yield $[Ru(S_2C\text{-}DO3A\text{-}^tBu)(dppm)_2]PF_6$ (**2**). Initially, the reaction was stirred at room temperature; however, this led to incomplete reaction, probably due to difficulty in accommodating the steric bulk of the pendant CH_2Bu^t groups. Gentle heating yielded the pale yellow product (**2**) in 84% yield (Scheme 2). Little change was observed in the solid state IR spectrum compared to that of the free ligand (**1**) with $\nu_{C=O}$ and ν_{C-O} absorptions observed at 1725 and 1152 cm^{-1}, respectively. The resonances due to the macrocycle were observed as a series of multiplets between 2.3 and 4.2 ppm in the ^{1}H NMR spectrum, while the methylene protons of the dppm ligands appeared as a broad multiplet between 4.28 and 4.64 ppm. These resonances integrated correctly with those for the tertiarybutyl groups between 1.30 and 1.71 ppm. The ^{31}P NMR spectrum provided information on the structural ramifications of introducing such a bulky dithiocarbamate ligand. The distortion of the usual octahedral geometry found in such dithiocarbamate complexes was evidenced by an effect on the equivalence of the phosphorus nuclei. The multiplet resonance observed at −5.5 ppm was assigned to the equatorial phosphorus nuclei while two smaller triplet resonances at −18.6 and −20.5 ppm were attributed to the axial phosphorus nuclei. An abundant molecular ion was observed at m/z 1459 in the mass spectrum (fast atom bombardment, positive mode) while elemental analysis data were in good agreement with calculated values for the proposed formulation.

Treatment of a deep red solution of the Ru(II) vinyl compound $[Ru(CH{=}CHC_6H_4Me\text{-}4)Cl(BTD)(CO)(PPh_3)_2]$ with 1 equiv of DO3A-^{t}Bu-CS_2K in chloroform rapidly led to a yellow solution, indicating the loss of the BTD (2,1,3-benzothiadiazole) ligand to form $[Ru(CH{=}CHC_6H_4Me\text{-}4)(S_2C\text{-}DO3A\text{-}Bu^t)(CO)(PPh_3)_2]$ (**3**), as shown in Scheme 2. A singlet at 39.5 ppm in the ^{31}P NMR spectrum confirmed the generation of a new product and confirmed the phosphine ligands to adopt a mutually *trans* arrangement. The infrared spectroscopic data (solid state) associated with the dithiocarbamate ligand differed little from that found in the spectrum of **2** apart from an intense ν_{CO} absorption at 1914 cm^{-1}. The ^{1}H NMR spectrum showed significant chemical inequivalence between the ester groups and between the NCH_2 protons of the DO3A-^{t}Bu-CS_2 ligand. The interactions between the CH_2 protons closest to the dithiocarbamate led to well-defined triplets showing a coupling of 5.8 Hz. The alkenyl α-proton appeared as a doublet of triplets with strong coupling to Hβ (J_{HH} = 16.8 Hz) and longer range coupling to the two equivalent phosphorus nuclei (J_{HP} = 3.2 Hz). The aromatic protons of the tolyl substituent gave rise to an AB coupling system (J_{AB} = 7.9 Hz) at 6.35 and 6.82 ppm, while the methyl proton was found to resonate at 2.23 ppm. The formation of **3** was confirmed by a molecular ion at m/z 1360 in the FAB mass spectrum. Good agreement was found between calculated and determined elemental analysis values, confirming the overall composition of the product.

The focus of the reactivity studies with **1** was then moved from octahedral complexes to square planar systems based on group 10 metals. The reaction between $[Pd(C,N\text{-}C_6H_4CH_2NMe_2)Cl]_2$ and 2 equiv of **1** occurred rapidly to yield a pale yellow solid in good yield (91%), as shown in Scheme 2. The successful formation of a new product rested largely on the ^{1}H NMR spectrum, which displayed a multiplet between 3.93 and 4.03 ppm for the CH_2 protons of the cyclometalated chelate as well as a singlet at 2.89 ppm (NMe_2). The protons in α- and β-positions to the dithiocarbamate nitrogen were rendered inequivalent, giving rise to closely spaced triplets at 3.09 and 3.14 ppm and multiplets between 4.13 and 4.33 ppm, respectively. Elemental analysis and mass spectrometry data confirmed the formulation as $[Pd(C,N\text{-}C_6H_4CH_2NMe_2)(S_2C\text{-}DO3A\text{-}Bu^t)]$ (**4**). A Pt(II) example was prepared by reaction of **1** and $[PtCl_2(PPh_3)_2]$ in the presence of excess NH_4PF_6. The reaction was stirred at room temperature for 16 h (Scheme 2) to yield the cationic product $[Pt(S_2C\text{-}DO3A\text{-}Bu^t)(PPh_3)_2]PF_6$ (**5**). The ^{31}P NMR spectrum contained a singlet at 14.8 ppm (J_{PPt} 3293 Hz). The ^{1}H NMR spectrum of the product displayed typical resonances for the DO3A-^{t}Bu-CS_2 ligand, which integrated correctly with the aromatic resonances for the PPh_3 ligands. The formulation was further supported by a 100% abundant molecular ion at m/z 1309 in the FAB mass spectrum (+ve mode).

Examples of linear complexes bearing the DO3A-^{t}Bu-CS_2 ligand were provided by reaction of $[AuCl(PR_3)]$ (R = Ph, Cy) with **1** to yield $[Au(S_2C\text{-}DO3A\text{-}Bu^t)(PPh_3)]$ (**6**) and $[Au(S_2C\text{-}DO3A\text{-}Bu^t)(PCy_3)]$ (**7**), as shown in Scheme 2. In complex **6**, two ν(C−S) bands at 997 and 968 cm^{-1} were observed, suggesting that the dithiocarbamate ligand was coordinated in a monodentate binding mode, as is typically found in Au(I) dithiocarbamate compounds. The remaining spectroscopic data associated with the dithiocarbamate ligand in both complexes were similar to those found for compounds **2**−**5**. Mass spectrometry analysis of the compounds revealed molecular ions at m/z 1049 (**6**) and m/z 1067 (**7**), confirming the overall composition of the products, in conjunction with elemental analysis.

Homoleptic Complexes. Having probed the reactivity of the DO3A-^{t}Bu-CS_2 ligand (**1**) with a range of metal complexes of differing geometries and bearing other coligands (allowing characterization through internal integration of their ^{1}H NMR features), attention turned to the generation of homoleptic species. In terms of potential as contrast agents for MRI, these compounds are the most interesting as they allow up to three macrocycles to be incorporated into the same molecular assembly. Since each macrocycle can accommodate a metal ion, three Gd(III) centers can be arranged around a central transition metal ion. As described above, this approach has already received some attention; however, to date, no reports have appeared in which dithiocarbamate linkages have been explored.

The methods used by many researchers for their transition metal centered self-assemblies involved initial formation of the Gd(III) chelate, followed by formation of the octahedral complex.[16,18,19,21,47] The opposite approach was employed in this work, making use of the soft−soft affinity of the transition

dx.doi.org/10.1021/ic401936w | Inorg. Chem. 2014, 53, 1989−2005

Scheme 3. Formation of Homoleptic Bis(dithiocarbamate) Complexes[a]

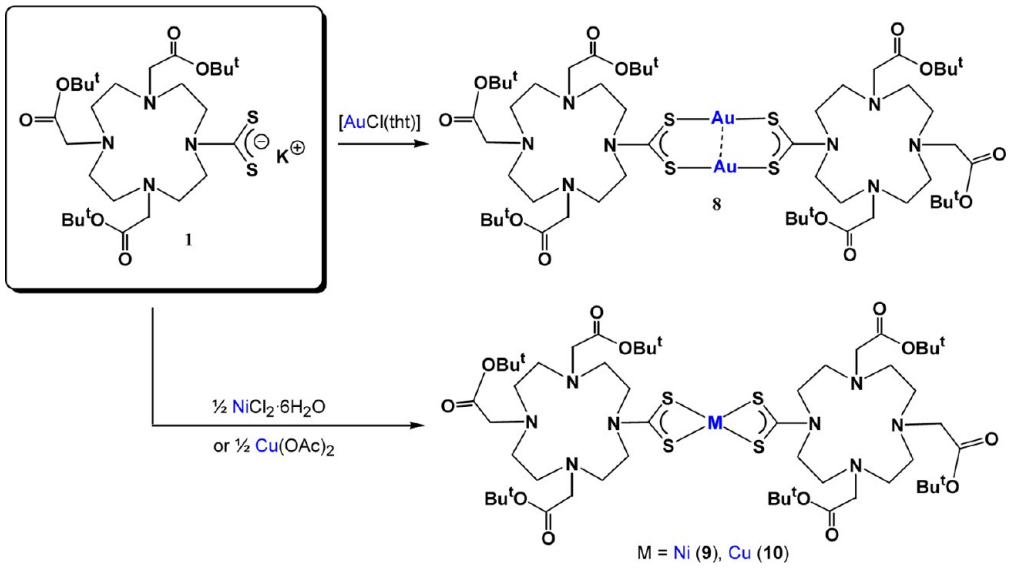

[a]tht = tetrahydrothiophene.

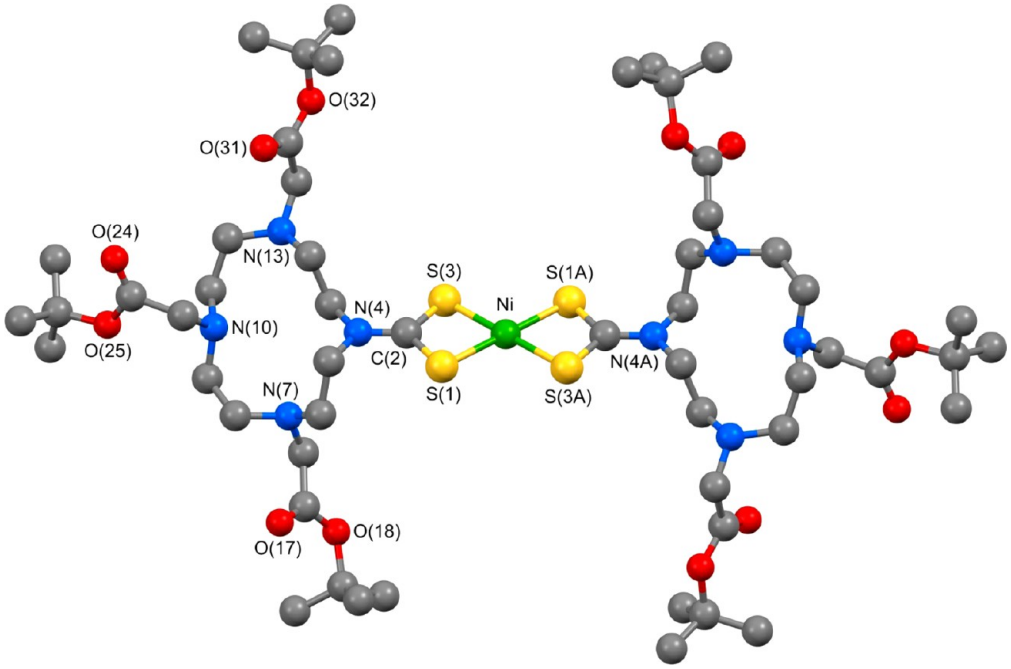

Figure 2. Crystal structure of the C_i-symmetric complex **9**. Atoms labeled with an "A" after the number are related to their counterparts without the letter by the center of symmetry situated at the nickel center. Selected bond lengths (Å) and angles (deg): Ni–S(1) 2.1976(4), Ni–S(3) 2.2045(4), S(1)–C(2) 1.7184(16), C(2)–S(3) 1.7282(16), C(2)–N(4) 1.313(2), S(1)–Ni–S(3) 79.621(15), S(1)–C(2)–S(3) 109.71(9).

metal core for the dithiocarbamate ligand (**1**), before deprotection of the ester groups and subsequent chelation of the Gd(III) ions. Deprotection of the *tert*-butyl ester groups is typically achieved using trifluoroacetic acid, which risked reverting the dithiocarbamate moiety back to its constituent amine and carbon disulfide.[48] However, when dithiocarbamates are coordinated to a transition metal center, their stability toward acids is greatly improved.[25]

A dinuclear Au(I) species, $[Au_2(S_2C\text{-}DO3A\text{-}Bu^t)_2]$ (**8**), was obtained in good yield by stirring equimolar solutions of [AuCl(tht)] (tht = tetrahydrothiophene) and dithiocarbamate **1** at room temperature (Scheme 3). The solid appeared to be indefinitely air and moisture stable as a solid at room temperature; however, in solution the compound was susceptible to formation of gold colloid. The infrared spectrum showed typical absorptions for the dithiocarbamate ligand, although the ν_{C-N} band in **8** (1481 cm^{-1}) was found to have increased in frequency, compared to the corresponding value for the dithiocarbamate ligand **1** (1453 cm^{-1}), indicating a greater degree of C–N multiple bond character. The chemical shifts observed in the ^1H NMR spectrum of **8** were similar to those found for **1** so the formulation rested largely on the FAB mass spectrum (100% abundant molecular ion at m/z 1573)

dx.doi.org/10.1021/ic401936w | *Inorg. Chem.* 2014, 53, 1989–2005

Scheme 4. Formation of a Homoleptic Tris(dithiocarbamate) Complex

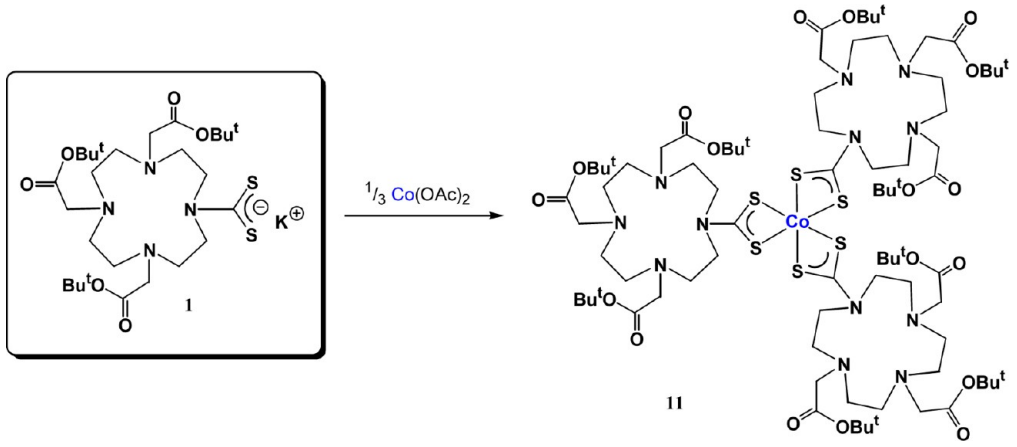

Scheme 5. Deprotection of Ester Groups and Coordination of Lanthanide Ions

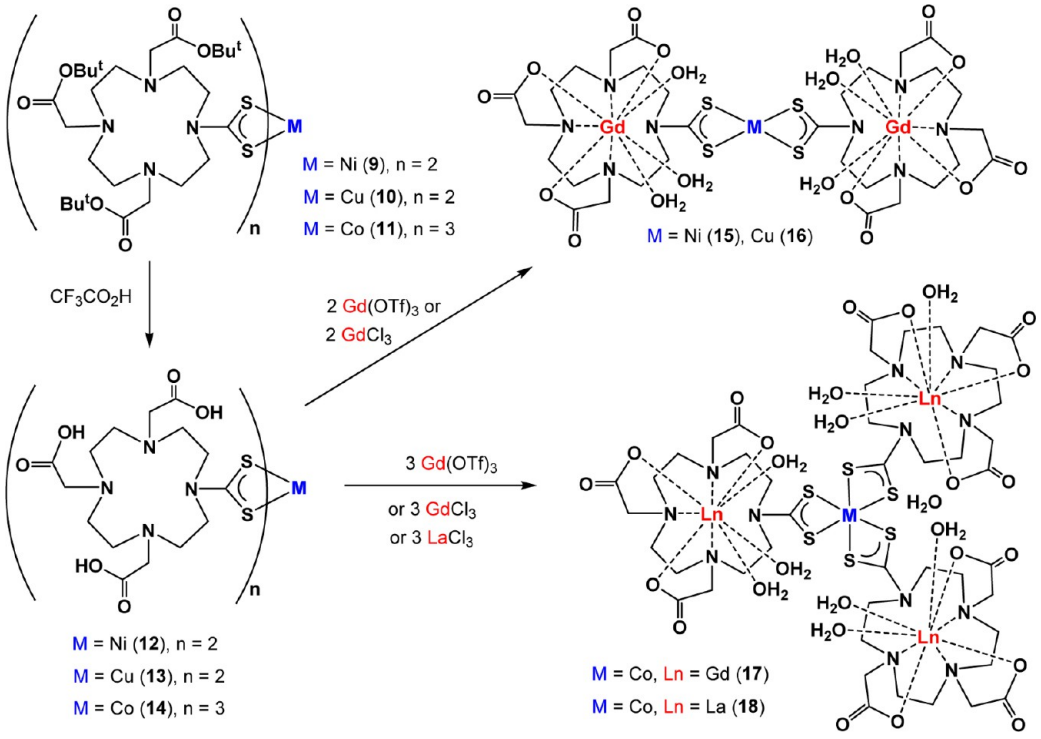

and good agreement of elemental analysis data with calculated values.

Due its instability in solution, compound **8** proved unsuitable for the ultimate goal of coordination of Gd(III) ions so the focus moved to the reactions of DO3A-^{t}Bu-CS_2K (**1**) with nickel and copper precursors. Nickel bis(dithiocarbamate) complexes have been known for over a century,[25,49] and the complex [Ni(S_2C-DO3A-Bu^t)$_2$] (**9**) formed readily on reaction of 2 equiv of **1** with $NiCl_2 \cdot 6H_2O$. The green product was obtained in 70% yield, and as with compound **8**, the lack of significant spectroscopic change (^{1}H NMR and IR spectroscopies) on coordination of the dithiocarbamate led to ^{13}C NMR being employed. The diagnostic low-field resonance of the quaternary CS_2 nucleus was observed to be shifted upfield to 205.6 ppm from the position observed in the spectrum of **1**. Mass spectrometry analysis (FAB, +ve mode) revealed an abundant molecular ion at m/z 1237, while elemental analysis further supported the proposed composition of the green product. Single crystals of **9** were grown by layering a solution of the complex in dichloromethane with methanol (Figure 2) to allow characterization of **9** to be completed by an X-ray crystallography study. Interestingly, on closer inspection the crystals appeared both red and green under different light conditions, which is consistent with the previous observation of green−red dichroic platelets of nickel(II) bis[(aza-15-crown-5)dithiocarbamate].[50]

The nickel center was found to have a distorted square planar geometry with a S(1)−Ni−S(3) chelate bite angle of angle of 79.621(15)°. The Ni−S(1) and Ni−S(3) bond lengths of 2.1976(4) and 2.2045(4) Å, respectively, are slightly different from each other, but within the range typically observed for Ni(II) bis(dithiocarbamate) complexes.[25] The C(2)−N(4) bond length of 1.313(2) Å indicates a significant degree of double bond character,[51] in agreement with the high ν(C−N)

dx.doi.org/10.1021/ic401936w | Inorg. Chem. 2014, 53, 1989−2005

frequency observed using infrared spectroscopy. This significant double bond character also causes the NiS_2CNC_2 moiety to be almost completely flat, the {Ni,S(1),C(2),S(3),N(4),-C(5),C(15)} atoms being coplanar to within ca. 0.03 Å.

A further example of a bis(dithiocarbamate) complex was prepared from the reaction of 2 equiv of **1** with $Cu(OAc)_2$. The paramagnetic product was formulated as $[Cu(S_2C\text{-}DO3A\text{-}Bu^t)_2]$ (**10**) on the basis of infrared, mass spectrometry, and elemental analysis data. Copper bis(dithiocarbamate) complexes are well-known and often display distorted square planar geometry.

Co(III) tris(dithiocarbamate) complexes can be synthesized from Co(II) or Co(III) salts with 3 equiv of a dithiocarbamate salt. In the former case, Co(II) bis(dithiocarbamate) complexes form initially before spontaneous aerial oxidation yields the Co(III) complexes. A particularly relevant example is the tris(dithiocarbamate) complex based on an aza-15-crown-5 dithiocarbamate ligand.[50] The compound $[Co(S_2C\text{-}DO3A\text{-}Bu^t)_3]$ (**11**) resulted from the rapid reaction between 1 equiv of Co(II) acetate tetrahydrate and 3 equiv of **1** and was obtained as a dark green solid in 89% yield (Scheme 4). ^{1}H NMR analysis revealed the expected resonances for the dithiocarbamate ligand with no evidence of broadening suggesting that the Co(III) center was low spin d^6. The ^{1}H NMR spectrum displayed triplet resonances for the ethylene protons closest to the dithiocarbamate nitrogen with identical J_{HH} coupling constants of 5.3 Hz at 4.05 and 3.10 ppm. This indicated that the compound was highly symmetrical and also that the Λ- and Δ-enantiomers were spectroscopically indistinguishable. A multiplet centered at 2.77 ppm accounted for 24 NCH_2 protons while the resonances at 3.34 and 1.47 ppm were assigned to the remaining methylene protons and those of the methyl groups. The ^{13}C NMR spectrum revealed a characteristic low-field CS_2 carbon resonance at 204.8 ppm. Mass spectrometry (FAB) displayed an abundant molecular ion at m/z 1828 while elemental analysis also confirmed the composition of the product.

Deprotection and Coordination of Gadolinium. The next phase of the investigation was to ascertain whether conversion of the ester groups to carboxylic acid functionality could be achieved without compromising the dithiocarbamate linkage (cf., acid sensitivity of uncoordinated dithiocarbamates[25]). Tertiary butyl esters are selectively cleaved using trifluoroacetic acid to yield the corresponding acids in a widely used protocol. In each case, the $[M(S_2C\text{-}DO3A\text{-}Bu^t)_n]$ (n = 2, 3) complex was dissolved in a mixture of dichloromethane and trifluoroacetic acid (3:1 ratio by volume) and stirred at room temperature for 45−60 h. This led to complete deprotection in all cases without evidence of undesired reaction at the 1,1-dithio chelate.

Using this method, $[Ni(S_2C\text{-}DO3A\text{-}Bu^t)_2]$ (**9**) was converted into $[Ni(S_2C\text{-}DO3A)_2]$ (**12**) in 98% yield (Scheme 5). The color of the solution remained constant throughout the reaction, suggesting that no significant change had taken place at the metal center or dithiocarbamate linkage as a result of the acidic solution. This transformation resulted in the generation of six carboxylic acid units, rendering complex **12** insoluble in dichloromethane and moderately soluble in alcohols and water. The infrared spectrum (solid state) indicated that deprotection to form the carboxylic acid had been successful due to the appearance of a broad ν_{O-H} absorption at 3401 cm^{-1}. The remaining carboxylic acid $\nu_{C=O}$ and ν_{C-O} absorptions were still present, as were the ν_{C-N} and ν_{C-S} bands attributed to the dithiocarbamate ligand. ^{1}H NMR analysis showed broad resonances with the correct integrals for the DO3A-CS_2 ligand and an absence of methyl (Bu^t) resonances in the high field region. The overall formulation was supported by a molecular ion at m/z 901 in the mass spectrum (FAB, +ve mode) and good agreement of elemental analysis with calculated values.

An identical procedure ensured conversion of $[Cu(S_2C\text{-}DO3A\text{-}Bu^t)_2]$ (**10**) to $[Cu(S_2C\text{-}DO3A)_2]$ (**13**) in quantitative yield. Similar spectroscopic data (apart from the effect of the paramagnetic center) were observed as seen for the nickel analogue (**12**).

Reaction of $[Co(S_2C\text{-}DO3A\text{-}Bu^t)_3]$ (**11**) under the same conditions yielded $[Co(S_2C\text{-}DO3A)_3]$ (**14**) in 88% yield (Scheme 5). Again, the solution remained green during the reaction, confirming the stability of the dithiocarbamate complex **14** in acidic condition. The product only showed substantial solubility at room temperature in polar solvents such as water and dimethyl sulfoxide. The solid state infrared spectrum displayed a new absorption at 3409 cm^{-1} for the ν_{O-H} mode. ^{1}H NMR analysis of the product in D_2O gave broad resonances that integrated correctly for the proposed formulation. Further analytical data confirmed the formulation of the complex.

Heating a mixture of a lanthanide(III) salt and the DOTA-derivative is often used to form the encapsulated lanthanide complexes. However, a milder route was also employed in this study involving stirring a solution of the compounds at room temperature for 24 h. After precipitation of the products, thorough washing of the solid was employed to remove uncoordinated metal ions. The greater affinity of lanthanides for harder donor atoms strongly disfavored cleavage of the transition metal-dithiocarbamate bonds by the Gd(III) ions.[52,53]

The reaction of $[Ni(S_2C\text{-}DO3A)_2]$ (**12**) with 2 equiv of gadolinium(III) chloride (or triflate salt) led to a color change after 24 h (Scheme 5) and resulted in the isolation of a yellow-orange solid, $[Ni(S_2C\text{-}DO3A\text{-}Gd)_2]$ (**15**). Compared to the precursor (**12**), the product was readily soluble in methanol but was still insoluble in chlorinated solvents. The unresolved features in the ^{1}H NMR spectrum of **15** confirmed the paramagnetic nature of the complex. The mass spectrum (FAB, +ve mode) of the sample revealed a molecular ion peak at m/z 1212 which also displayed the correct isotopic distribution patterns. The relatively high frequency of the dithiocarbamate ν_{C-N} absorption at 1490 cm^{-1} implied a high bond order for the C−N bond due to the contribution of the nitrogen lone pair. This suggested that there is little or no interaction between the dithiocarbamate nitrogen and the Gd(III) ion, implying that the lanthanide ion was coordinated to only six donors of the DO3A chelate. An infrared ν_{O-H} absorption at 3358 cm^{-1} indicated that water molecules were also bound to the Gd(III) ion. The ν_{O-C-O} absorptions were observed at 1594 and 1254 cm^{-1}, falling in the frequency range typical for the expected ionic binding mode to lanthanide ions.[54]

Infrared ν_{C-N} and structural data (for **9**) showed that substantial multiple bond character was likely to be present in all the complexes described here (rendering the R_2NCS_2 unit planar). Given the coordination of the three carboxylate arms and the evidence for a hydration number of 3 (*vide infra*), tridentate coordination was assumed for the nitrogen donors of the macrocyle (Scheme 5) in order to achieve the usual coordination number of 9. This is further supported by the

dx.doi.org/10.1021/ic401936w | Inorg. Chem. 2014, 53, 1989−2005

marked lack of literature examples of dithiocarbamate complexes in which the nitrogen coordinates to a metal.[25c] Despite repeated attempts, crystals of sufficient quality for X-ray diffraction could not be obtained of any of the d−f hybrids. Although no examples are known for hexadentate coordination of directly comparable chelates, the flexibility of the ethylene bridges is well established in such macrocycles (and crown ethers etc.). When considered alongside the lack of orbital-based directionality in lanthanide chelation, this strongly suggests that hexadentate coordination through three nitrogen donors and the three carboxylate arms is feasible.

In a similar manner, $[Cu(S_2C\text{-}DO3A)_2]$ (**13**) was converted into $[Cu(S_2C\text{-}DO3A\text{-}Gd)_2]$ (**16**) through reaction with 2 equiv of $Gd(OTf)_3$. A better yield was obtained for this dark brown product compared to the analogous nickel example (**15**). Infrared spectroscopic data for **16** were found to be similar to those recorded for **15**.

Stirring $[Co(S_2C\text{-}DO3A)_3]$ (**14**) with 3 equiv of $Gd(OTf)_3$ in water for 24 h at room temperature led to formation of dark green $[Co(S_2C\text{-}DO3A\text{-}Gd)_3]$ (**17**) in 65% yield. Mass spectrometry (FAB) revealed a molecular ion at m/z 1787. The infrared spectrum of **17** displayed a relatively high ν_{C-N} absorption frequency, indicating a significant degree of C−N double bond character. This suggested that, as with **15** and **16**, there was no significant interaction between this nitrogen and the Gd(III) ion, providing multiple solvent coordination sites. The infrared spectrum of a sample of **17** (crystallized from wet methanol) supported this hypothesis through the presence of a ν_{O-H} absorption at 3393 cm^{-1} assigned to coordinated water. The coordinated water is lost on drying under high vacuum, as shown by the observed elemental analysis data. Trans-metalation experiments with Zn(II) indicated reasonable kinetic stability for the multimetallic complexes, though lower than that observed for DOTA-Gd (Supporting Information), which displays octadentate coordination to the metal ion. While this degree of stability is encouraging, cell studies would be needed in order to determine stability and performance of the compounds reported here in a biological environment.

In order to obtain further data on this type of tetrametallic assembly, the analogous $CoLa_3$ complex was prepared by treating $[Co(S_2C\text{-}DO3A)_3]$ (**14**) with 3 equiv of $LaCl_3$ to form the diamagnetic La(III) (f^0) complex $[Co(S_2C\text{-}DO3A\text{-}La)_3]$ (**18**) in excellent yield. The dark green compound displayed moderate solubility in water and was insoluble in alcohols. The ^1H NMR spectrum of **18** showed the methylene protons of the α-carbons resonating at 4.08 ppm while the CH_2CO_2 protons gave rise to two partially overlapping singlet peaks at 3.68 ppm. The methylene protons of the β-carbons were observed at 3.49 ppm, and the remaining NCH_2 protons gave a multiplet centered at 3.30 ppm. The multiplicities and chemical shifts observed in **18** were almost identical to those found in the spectrum of the precursor (**14**), which indicated that the binding of lanthanum(III) had little effect on the chemical environment of the rest of the molecule. The infrared spectrum of **18** displayed a strong, broad ν_{O-H} absorption at 3303 cm^{-1}, indicating bound water at the lanthanum(III) center. The remaining infrared absorptions were similar to those observed for **17**, confirming that the two complexes were likely to be structurally similar. Elemental analysis data were found to be in good agreement with the proposed formulation of **18** (Scheme 5).

In the transformations from ester to carboxylic acid to Gd(III) chelate, infrared spectroscopy proved to be particularly diagnostic. For each compound (i) the formation of a broad ν_{O-H} absorption was observed on formation of the tricarboxylic acid, and (ii) a large reduction was noted in the frequency of the intense absorption for $\nu_{C=O}$ in the triacid to become the asymmetric ν_{O-C-O} absorption in the Gd(III) complex and (iii) the increase in frequency of the ν_{C-O} band on going from triester to triacid. The dithiocarbamate ν_{C-N} and ν_{C-S} absorption bands also remained approximately constant throughout the entire series of compounds which implied that the bonding to the transition metal remained unaffected by the transformations of the macrocycles.

In order to explore the properties of the gadolinium complexes, relaxivity studies were undertaken at 400 MHz (9.4 T). Compound **16** (Cu) gave a value of r_1 = 11.0 mM^{-1} s^{-1} per Gd center and r_1 = 22.0 mM^{-1} s^{-1} per object while **17** (Co) showed an r_1 value of 11.5 mM^{-1} s^{-1} per Gd center and r_1 = 34.5 mM^{-1} s^{-1} per object. These relaxation rates are in the typical range for complexes with hydration number (q) of 3, which has been shown by Mazzanti and co-workers for their dpaa ligand system.[55] In bidentate dithiocarbamate complexes, the nitrogen lone pair is involved substantially in the C−N bond, such that there is significant multiple bond character. This renders the R_2NCS_2M unit coplanar, as observed in the structure of **9**. This involvement is likely to preclude the interaction of the nitrogen lone pair with additional metal centers.[25] This aspect has been exploited in the ring-closing metathesis of coordinated diallyldithiocarbamate ligands,[3e] which contrasts with the deactivation of the catalyst in the presence of the parent diallylamine due to coordination. The hydration number of q = 3 is also supported by lifetime measurements carried out for the functionalized nanoparticles (*vide infra*): fluorescence spectra of Eu and Tb analogues of the multimetallic species exhibited very low emission intensities. From these observations, it is assumed that the dithiocarbamate nitrogen in **16** and **17** does not coordinate to the gadolinium center, leading to the high q and r_1 values. The slight difference in r_1 values between **16** and **17** could be due to the increase in mass of the agent (2 vs 3 Gd centers). It must be noted that these compounds would bind endogenous anions, such as carbonate and phosphates, due to the charge and large hydration state; studies on neutral Gd(III) chelates with 2 and 3 bound waters, have shown high affinities for endogenous anions and are well described in literature.[56]

Nanoparticle Functionalization. The results described above demonstrated the utility of the DO3A-CS_2K (**1**) ligand in the formation of mixed transition metal−lanthanide compounds. The focus of the study then moved to using the same methodology to functionalize gold nanoparticles with **1**. Recent work by ourselves[4] and others[43,57] has shown that dithiocarbamates provide a versatile alternative to the ubiquitous thiols for surface functionalization of gold nanoparticles,[58] offering advantages such as a more straightforward synthetic approach and stronger attachment to the gold surface.

Two different methods for the preparation of gold nanoparticles were employed. The citrate method[59] is based on the Turkevich protocol[60] and involves initial reduction of an Au(III) precursor with sodium citrate before addition of the sulfur surface unit to displace the citrate groups. The nanoparticles produced are typically 15−20 nm in diameter. The Brust−Schiffrin method[61,62] proceeds through reduction of $[AuCl_4]^-$ with sodium borohydride in the presence of the sulfur surface unit, resulting in smaller nanoparticles between 2 and 5 nm in diameter.

dx.doi.org/10.1021/ic401936w | Inorg. Chem. 2014, 53, 1989−2005

Scheme 6. Functionalization of the Surface of Gold Nanoparticles with DO3A-CS_2 Surface Units

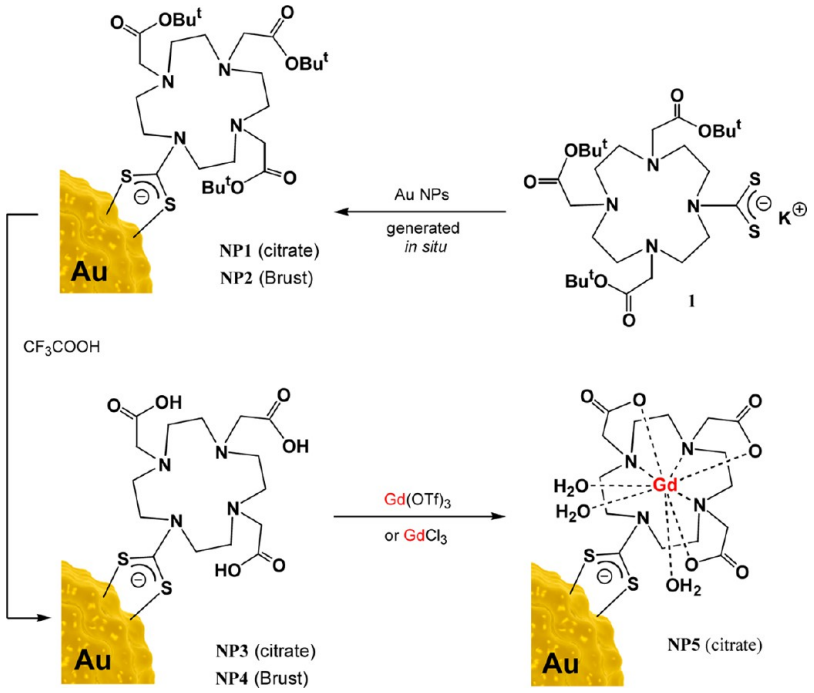

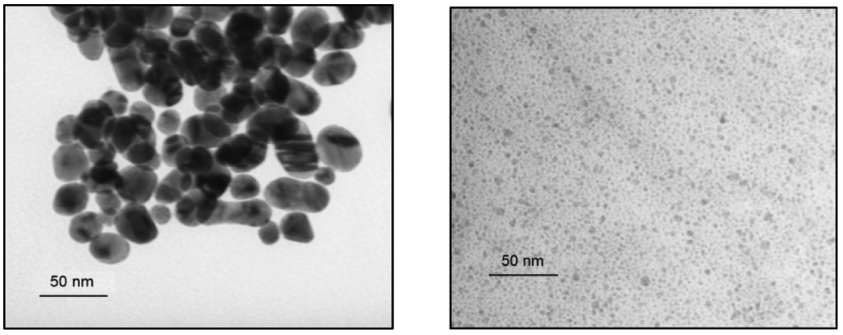

Figure 3. TEM images of **NP1** (left, 19.7 ± 3.7 nm) and **NP2** (right, 3.7 ± 1.0 nm).

An aqueous solution of $HAuCl_4$ was reduced using trisodium citrate to produce a ruby red solution. Addition of **1** to the reaction mixture (Scheme 6) caused precipitation of a fine black powder, indicating the formation of dithiocarbamate-functionalized nanoparticles, [Au@S_2C-DO3A-^{t}Bu] (**NP1**). The nanoparticles were isolated by centrifuging before being washed repeatedly with water to remove unattached dithiocarbamate surface units and free citrate ions. This process was continued until analysis (^{1}H NMR and infrared spectroscopy) of the washings revealed no signals for these species.

^{1}H NMR analysis of the black powder (**NP1**) revealed triplets at 4.42 and 3.18 ppm which were assigned to the protons of the α-carbons. The resonances of these protons were found to be broadened and shifted to higher field compared to the same frequencies in the dithiocarbamate **1**. The presence of metal colloids in liquid-phase NMR samples can create large inhomogeneities in the magnetic field of local chemical environments,[31] so these chemical shift values and broadened signals were taken to be indicative of successful attachment of the dithiocarbamate to the surface of the gold nanoparticle. Less pronounced broadening was also observed in the resonances of the protons of the β carbons at 3.10 ppm. A multiplet between 2.74 ppm and 2.84 ppm accounted for the remaining protons of the DO3A backbone, while resonances for the *tert*-butyl protons were observed between 1.45 and 1.47 ppm. The solid state infrared spectrum displayed similar features for both **NP1** and the free dithiocarbamate **1**, confirming the presence of the dithiocarbamate on the surface of the gold nanoparticles. A shift to lower frequency was observed for the ν_{C-S} absorption while the dithiocarbamate ν_{C-N} band remained essentially unaffected by the formation of nanoparticles at 1455 cm^{-1}. No absorptions due to residual citrate ions were observed in the infrared spectrum. The nanoparticles produced (**NP1**) showed excellent stability toward the atmosphere and could be redispersed in organic solvents such as chloroform and acetone. Transmission electron microscopy (TEM) was used to image the nanoparticles (Figure 3) and allowed the average diameter to be calculated (19.7 ± 3.7 nm). Energy dispersive X-ray spectroscopy (EDS) was also employed to analyze **NP1** and revealed that sulfur was present as well as gold, while nitrogen, carbon, and oxygen could not be differentiated with confidence. Importantly, no trace of potassium countercations was indicated by the EDS measurements. This is in agreement with a recent computational study, which suggested the anionic charge of the surface

dx.doi.org/10.1021/ic401936w | *Inorg. Chem.* 2014, 53, 1989−2005

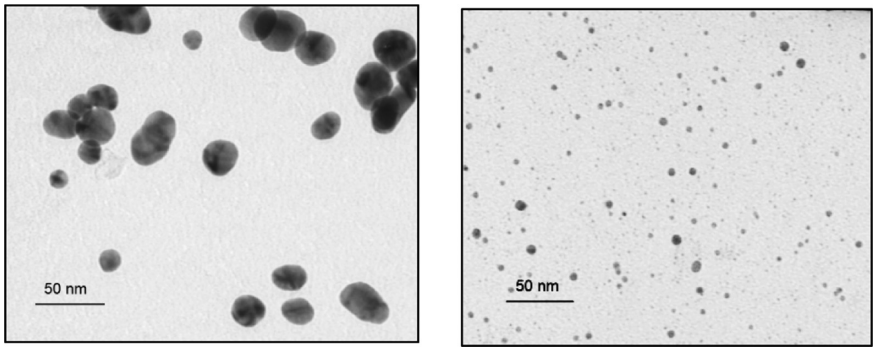

Figure 4. TEM images of **NP3** (left, 18.9 ± 4.8 nm) and **NP4** (right, 3.7 ± 0.9 nm).

unit is balanced by partial positive charge on the gold atoms to which the dithiocarbamate is attached.[44]

The ability to control the size of the nanoparticles has significant potential in a medical setting, not least in the ability of the nanoparticulates to pass through certain membranes in the body (e.g., blood−brain barrier). In addition, the surface area will be significantly different as will the number of surface units. For these reasons, the Brust−Schiffrin method[61] was employed to access nanoparticles in a smaller size range. A phase transfer agent, tetraoctylammonium bromide (TOAB), is typically employed in order to transfer the Au(III) ions into the organic phase. Aqueous $HAuCl_4$ was treated with a chloroform solution of TOAB before the organic layer was isolated. Dithiocarbamate **1** was added, and the sodium borohydride reducing agent was added dropwise at low temperature causing the reaction mixture to change from yellow to dark brown. However, the product showed substantial agglomeration, making it difficult to isolate. Infrared analysis indicated that the phase transfer agent (TOAB) was still present, and this proved difficult to remove through washing. In order to avoid the use of TOAB, a modification to the method[62] was employed in which a solution of $HAuCl_4$ in methanol was prepared and an aqueous solution of DO3A-CS_2K (**1**) added directly to the reaction mixture (Scheme 5). This created a single phase system which avoided the need to extract gold(III) ions into the organic layer. Addition of sodium borohydride led to the solution becoming brown, indicating the formation of the gold nanoparticles, Au@S_2C-DO3A-^{t}Bu (**NP2**). While a 3:1 gold/ligand ratio is commonly used for simple, linear thiols, a 1:1 ratio of gold to ligand was used in this work. This follows the approach of Roux and co-workers, who used similar sized surface units to those employed here.[34,35] The modified method showed a marked improvement, with the infrared spectrum displaying characteristic absorptions for the dithiocarbamate surface units. As observed for **NP1**, the infrared absorptions associated with dithiocarbamate **1** were maintained in **NP2**, while ^{1}H NMR spectroscopic analysis further supported the presence of the surface units with similar resonances being observed to those identified for **NP1**. The formation of gold nanoparticles with an average particle size of 3.7 ± 1.0 nm (Figure 3) was confirmed by TEM analysis, while EDS data also indicated the presence of sulfur on the surface of the nanoparticles.

Before coordination of lanthanide ions could be attempted, conversion of the tertiarybutyl ester groups to the corresponding carboxylic acid was necessary. This was achieved using a similar procedure to that employed for the molecular complexes mentioned above using trifluoroacetic acid (TFA). The reaction and workup procedures for the deprotection were based on those in the literature.[63] Chloroform solutions of nanoparticles **NP1** and **NP2** were treated with excess trifluoroacetic acid over a 2−3 day period at room temperature (Scheme 6). The conversion was monitored by ^{1}H NMR spectroscopy. The product obtained from deprotection of **NP1**, Au@SC_2-DO3A (**NP3**), was washed thoroughly with chloroform to ensure that all TFA was removed. The increased solubility compared to the precursor of **NP3** in more polar solvents such as methanol and water indicated the effect of generating three carboxylic acid groups per chelate.

The nanoparticles prepared via the Brust−Schiffrin method (**NP2**) were also treated with TFA to afford the carboxylic acid derivative Au@S_2C-DO3A (**NP4**). Similar solubility changes were observed during the successive washes with chloroform; however, the **NP4** nanoparticles showed a less pronounced increase in solubility in polar solvents, perhaps due to the much smaller number of surface units on the smaller nanoparticles.

The deprotected nanoparticles were isolated by centrifuging and dried overnight under vacuum. In both cases, a small amount of gold metal appeared on the inside of the centrifuging tube, indicating that some degradation of the nanoparticles had taken place under the harsh conditions of the TFA reaction. The decomposition of dithiocarbamates under acid conditions is known to give the free amine and carbon disulfide.[25] This could result in loss of the dithiocarbamate from the surface of the nanoparticle. However, this process is much less favored for coordinated dithiocarbamate species, as observed in the successful generation of the multimetallic complexes **15**−**18** discussed above. Apart from the absence of the methyl resonances (^{t}Bu groups), only subtle differences were observed in the resonances in the ^{1}H NMR spectra of nanoparticles **NP3** and **NP4**. No resonance was observed at 11.5 ppm (corresponding to acidic proton of the TFA), suggesting that excess acid had been successfully removed by washing. Taking the infrared spectrum of **NP4** as an example, the presence of the carboxylic acid groups was confirmed through the observation of a broad ν_{O-H} stretch at 3368 cm^{-1} along with broadened $\nu_{C=O}$ and ν_{C-O} absorption bands at 1721 and 1146 cm^{-1}, respectively. The infrared spectrum also provided evidence for the presence of the dithiocarbamate linkage with absorptions at 1461 cm^{-1} (ν_{C-N}) and 992, 945 (ν_{C-S}).

The average particle size of the **NP3** nanoparticles calculated from the TEM images was 18.9 ± 4.8 nm, while the **NP4** nanoparticles were found to have an average diameter of 3.7 nm ± 0.9 nm (Figure 4). The TEM images clearly showed that the diameters of the nanoparticles were essentially unchanged from the triester precursors (**NP1** and **NP2**), indicating that

dx.doi.org/10.1021/ic401936w | Inorg. Chem. 2014, 53, 1989−2005

modification of the surface units does not significantly affect the mean gold core size.[42]

The next stage of the synthesis involved complexation of Gd(III) cations to form chelated complexes on the surface. A methanolic solution of **NP3** was stirred for 24 h with an excess of $Gd(OTf)_3$ or $GdCl_3$ (Scheme 6). The number of surface units was estimated[64] using the diameter from TEM measurements and the "footprint" of the DO3A-^{t}Bu-CS_2 surface unit taken from the structure of **9** (assuming 70% coverage[42]). All solvent was then removed under vacuum, and the nanoparticles were washed repeatedly with water to ensure that all uncoordinated metal ions were removed (determined by the xylenol orange test). Centrifuging was employed to isolate the nanoparticle product, Au@(S_2C-DO3A-Gd) (**NP5**), which was then dried overnight under vacuum. TEM analysis revealed the average diameter of the nanoparticles to be essentially unchanged from the precursor **NP3**, with a size of 18.6 ± 4.3 nm (Figure 5).

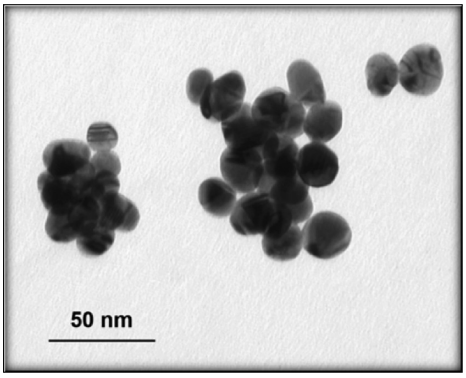

Figure 5. TEM images of **NP5** (left, 18.6 ± 4.3 nm).

^{1}H NMR analysis of the product showed significant broadening of the resonances assigned to water and the residual solvent peak in CD_3OD, taken as first indication of the presence of paramagnetic Gd(III) ions in the sample. Infrared analysis supported the formation of the metalated macrocycle with similar changes to those observed in the generation of the molecular $MGd_{2/3}$ species (**15**–**17**). Evidence of both monodentate ($\nu_{C=O}$ 1717 cm^{-1} and ν_{C-O} 1232 cm^{-1}) and ionic binding of the Gd(III) ions was observed as well as a broad ν_{O-H} absorption at 3387 cm^{-1} suggesting the presence of coordinated water molecules. The dithiocarbamate ν_{C-N} absorption was unaffected by the presence of the Gd(III) ions, implying little perturbation of the dithiocarbamate bonding. The presence of gadolinium as well as gold and sulfur was provided by EDS analysis. The efficacy of **NP5** as a contrast agent was assessed by relaxivity studies (at 400 MHz, 9.4 T). It was found to have an r_1 value of 4.8 mM^{-1} s^{-1} per Gd(III) center. On the basis of the same approximations of the number of Gd(III) units per nanoparticle used above (312 Gd(III) units at 70% coverage),[64] this corresponds to an overall r_1 value of 1498 mM^{-1} s^{-1} for **NP5**. This value per Gd(III) center is lower compared with **16** and **17** and is attributed to the effects of a high magnetic field on the larger object. This has also been recently observed by Mazzanti and co-workers when measuring the r_1 value of nanoparticle conjugates with chelates that have 3 bound waters at high field (200 MHz).[65] Furthermore, lifetime measurements were carried out with the Eu(III) analogue of **NP5** (**NP5-Eu**), in H_2O and D_2O, which confirm that 3 waters bind to metal center (see Supporting Information).

CONCLUSION

Although both dithiocarbamate ligands and polydentate chelates have been studied intensively, the ligand [DO3A-^{t}Bu-CS_2]$^-$ (**1**) is the first example of a polyfunctional dithiocarbamate linker, which can combine both d- and f-block ions within the same assembly. We have demonstrated that ligand **1** can be prepared readily and in high yield, making it an excellent starting point for multimetallic compounds. Coordination to a wide range of metals from the transition series showed that **1** reacts preferentially at the dithiocarbamate unit with all the metals explored, leaving the heterocyclic system available for coordination to Gd(III) ions after deprotection. Furthermore, the functionalization of gold nanoparticles can be achieved in a straightforward manner using a well-established methodology to provide robust [DO3A-^{t}Bu-CS_2]$^-$ surface units. Subsequent deprotection and functionalization with Gd(III) ions leads to functioning relaxivity agents. For the first time, dithiocarbamates have been employed in the construction of assemblies, which provide a platform for the design of potential MRI contrast agents. The next stage of the project will concentrate on cell studies to determine stability (in view of the reduced denticity compared to commercial agents) and performance of these agents in a biological environment.

EXPERIMENTAL SECTION

General Comments. All experiments were carried out under aerobic conditions, and the products obtained appear indefinitely stable toward the atmosphere, whether in solution or in the solid state. Solvents were used as received from commercial sources. The complexes $[Pd(C,NC_6H_4CH_2NMe_2)Cl]_2$,[66] [AuCl(tht)],[67] $[PtCl_2(PPh_3)_2]$,[68] $[AuCl(PPh_3)]$,[69] $[AuCl(PCy_3)]$,[70] and *cis*-$[RuCl_2(dppm)_2]$[71] were prepared using literature procedures. The complex $[Ru(CH{=}CHC_6H_4Me\text{-}4)Cl(BTD)(CO)(PPh_3)_2]$ was prepared using commercially available 2,1,3-benzothiadiazole (BTD) in place of the 2,1,3-benzoselenadiazole (BSD) in the literature procedure.[72] Petroleum ether refers to the fraction boiling in the range 40–60 °C. A Micromass AutoSpec Premier and Micromass LCT Premier instruments were used for collecting FAB and ESI mass spectrometry data, respectively. Infrared spectroscopy was performed using a Perkin-Elmer Spectrum 100 FT-IR spectrometer on solid samples. NMR spectroscopy data and T_1 relaxation measurements were obtained at 25 °C using a Bruker Avance 400 spectrometer. The resonances due to the PF_6^- anion in the ^{31}P NMR spectra were observed in the some of the cases below but are not reported. Elemental analyses were provided by London Metropolitan University. TEM images and EDS data were obtained using a JEOL 2010 high-resolution TEM (80–200 kV) equipped with an Oxford Instruments INCA EDS 80 mm X-Max detector system.

Preparation of DO3A-^{t}Bu-CS_2K (1). A mixture of [DO3A-^{t}Bu]-HBr (2.00 g, 3.358 mmol) and K_2CO_3 (3.71 g, 26.863 mmol) in acetonitrile (40 mL) was treated with carbon disulfide (0.20 mL, 3.358 mmol). The resultant yellow mixture was stirred for 1 h at room temperature, after which it was filtered to give a clear yellow solution. The solvent was removed under reduced pressure until a green-yellow foamy solid was present. The crude solid was dissolved in minimum chloroform and filtered through Celite to remove KBr and $KHCO_3$. The solvent was removed to yield the product as a yellow solid, which was dried under vacuum. Yield: 1925 mg (91%). IR (solid state): 2977, 2932, 2823 (ν_{C-H}), 1721 ($\nu_{C=O}$), 1453 (ν_{C-N}), 1366 (δ_{C-H}), 1222, 1151 (ν_{C-O}), 1112, 990 (ν_{C-S}), 969 (ν_{C-S}), 847, 751 cm^{-1}. ^{1}H NMR (400 MHz, $CDCl_3$): 1.45 (s, CH_3, 18H), 1.47 (s, CH_3, 9H), 2.33–3.30 (m, NCH_2 + CH_2COO^tBu, 12H + 6H), 3.92–4.62 (m, NCH_2, 2H),

dx.doi.org/10.1021/ic401936w | Inorg. Chem. 2014, 53, 1989–2005

5.38−6.40 (m, NCH_2, 2H) ppm. ^{13}C NMR (101 MHz, $CDCl_3$): 27.9 (s, CH_3), 28.1 (s, CH_3), 51.1 (s, NCH_2), 53.4 (s, NCH_2), 53.7 (s, NCH_2), 54.9 (s, NCH_2), 56.9 (s, CH_2COO^tBu), 57.7 (s, CH_2COO^tBu), 81.4 (s, $OCMe_3$), 81.9 (s, $OCMe_3$), 171.3 (s, C═O), 171.7 (s, C═O), 224.3 (s, CS_2) ppm. MS (ES −ve) *m*/*z* (abundance %) = 637 (31) $[M + 2Na]^-$. Anal. Calcd for $C_{27}H_{49}KN_4O_6S_2{\cdot}0.75CHCl_3$: C, 46.4; H, 7.0; N, 7.8%. Found: C, 46.0; H, 7.1; N, 7.8%.

Preparation of [Ru(S$_2$C-DO3A-^{t}Bu)(dppm)$_2$]PF$_6$ (2). A yellow solution of **1** (50 mg, 0.080 mmol) and *cis*-$[RuCl_2(dppm)_2]$ (75 mg, 0.080 mmol) in chloroform (20 mL) was treated with a solution of NH_4PF_6 (26 mg, 0.159 mmol) in methanol (10 mL) and heated at 50 °C for 10 min followed by stirring at room temperature for 3.5 h. All solvent was removed, and the resultant yellow residue was dissolved in minimum dichloromethane and filtered through Celite. The solution was evaporated to dryness and then triturated using ultrasound in diethyl ether (25 mL) to give a light yellow solid, which was filtered and dried under vacuum. Yield: 107 mg (84%). IR (solid state): 3056 (ν_{C-H}), 2978, 2939 (ν_{C-H}), 1725 ($\nu_{C=O}$), 1483 (ν_{C-N}), 1435, 1368 (δ_{C-H}), 1251, 1152 (ν_{C-O}), 1096, 1000 (ν_{C-S}), 831 (ν_{P-F}), 727, 694 cm^{-1}. ^1H NMR (400 MHz, CD_2Cl_2): 1.30−1.71 (m, CH_3, 27H), 2.37−4.16 (m, DO3A-^{t}Bu-CS_2 ligand, 22H), 4.28−4.64 (m, PCH_2, 2H), 4.77−5.06 (m, PCH_2, 2H), 6.34−8.33 (m, C_6H_5, 40H) ppm. ^{31}P NMR (162 MHz, CD_2Cl_2): −20.5 (t, *axial*-P, J_{PP} = 35.8 Hz), −18.6 (t, *axial*-P, J_{PP} = 33.5 Hz), −5.5 (m, *equatorial*-P) ppm. MS (FAB) *m*/*z* (abundance %) = 1459 (100) $[M]^+$. Anal. Calcd for $C_{77}H_{93}F_6N_4P_5O_6RuS_2{\cdot}CHCl_3$: C, 54.3; H, 5.5; N, 3.3%. Found: C, 54.1; H, 4.9; N, 2.8%.

Preparation of [Ru(CH═CHC$_6$H$_4$Me-4)(S$_2$C-DO3A-Bu^t)(CO)(PPh$_3$)$_2$] (3). A solution of $[Ru(CH{=}CHC_6H_4Me\text{-}4)Cl(BTD)(CO)(PPh_3)_2]$ (37 mg, 0.039 mmol) in chloroform (10 mL) was treated with a solution of **1** (50 mg, 0.080 mmol) in methanol (10 mL) and stirred at room temperature for 30 min. All solvent was evaporated and the residue was dissolved in minimum dichloromethane and filtered through Celite to remove KCl. All solvent was removed again, and pentane (2 × 10 mL) was added and then evaporated to ensure as much dichloromethane as possible was removed. The residue was then triturated in pentane (10 mL) for 20 min until a light yellow precipitate had formed. This was filtered and washed with pentane (10 mL) and then methanol (15 mL) followed by pentane (10 mL) again to remove BTD and unreacted **2**. The solid was then dried under vacuum. Yield: 26 mg (49%). IR (solid state): 3056 (ν_{C-H}), 2976, 2924, 2820 (ν_{C-H}), 1914 ($\nu_{C=O}$), 1725 ($\nu_{C=O}$), 1480 (ν_{C-N}), 1433, 1366 (ν_{C-H}), 1250, 1216, 1147 (ν_{C-O}), 1126, 1091, 999 (ν_{C-S}), 984, 844, 744, 693 cm^{-1}. ^1H NMR (400 MHz, $CDCl_3$): 1.46−1.48 (m, CH_3, 18H), 1.50−1.52 (m, CH_3, 9H), 2.23 (s, *p*-C_6H_4−CH_3, 3H), 2.52 (t, NCH_2, 2H, J_{HH} = 5.8 Hz), 2.58 (t, NCH_2, 2H, J_{HH} = 5.8 Hz), 2.60−2.72 (m, NCH_2, 8H), 3.13 (s, CH_2COO^tBu, 2H), 3.15 (s, CH_2COO^tBu, 2H), 3.23 (t, NCH_2, 2H, J_{HH} = 5.6 Hz), 3.27 (s, CH_2COO^tBu, 2H), 3.54 (t, NCH_2, 2H, J_{HH} = 5.9 Hz), 5.48 (d, Hβ, 1H, J_{HH} = 16.8 Hz), 6.35, 6.82 (AB, C_6H_4, 4H, J_{AB} = 7.9 Hz), 7.30−7.63 (m, C_6H_5, 30H), 7.71 (dt, Hα, 1H, J_{HH} = 16.8, J_{HP} = 3.2 Hz) ppm. ^{31}P NMR (162 MHz, $CDCl_3$): 39.5 (s, PPh_3) ppm. MS (FAB) *m*/*z* (abundance %) = 1360 (1) $[M]^+$, 1098 (50) $[M - PPh_3]^+$. Anal Calcd for $C_{73}H_{88}N_4O_7P_2RuS_2$: C, 64.4; H, 6.5; N, 4.1%. Found: C, 64.3; H, 6.4; N, 4.0%.

Preparation of [Pd(*C*,*N*-C$_6$H$_4$CH$_2$NMe$_2$)(S$_2$C-DO3A-Bu^t)] (4). A solution of $[Pd(C,N\text{-}C_6H_4CH_2NMe_2)Cl]_2$ (22 mg, 0.040 mmol) and **1** (50 mg, 0.080 mmol) in chloroform (10 mL) was stirred at room temperature for 1 h. All solvent was removed under reduced pressure, and the residue was then dissolved in minimum chloroform and filtered through Celite. As much solvent as possible was removed under removed pressure followed by repeated additions and evaporation of pentane (10 mL) until a pale yellow foamy product was produced. This was dried under vacuum. Yield: 60 mg (91%). IR (solid state): 3048 (ν_{C-H}), 2975, 2928, 2908, 2834 (ν_{C-H}), 1724 ($\nu_{C=O}$), 1503 (ν_{C-N}), 1366 (δ_{C-H}), 1147 (ν_{C-O}), 990 (ν_{C-S}), 848, 740 cm^{-1}. ^1H NMR (400 MHz, CD_2Cl_2): 1.49 (s, CH_3, 27H), 2.71−2.83 (m, NCH_2, 8H), 2.89 (s, $N(CH_3)_2$, 6H), 3.09 (t, $CH_2CH_2NCS_2$, 2H, J_{HH} = 5.6 Hz), 3.14 (t, $S_2CNCH_2CH_2$, 2H, J_{HH} = 5.6 Hz), 3.28−3.40 (m, CH_2COO^tBu, 6H), 3.93−4.03 (m, $C_6H_4CH_2$, 2H), 4.13−4.33 (m, CH_2NCS_2, 4H), 6.84−7.11 (m, C_6H_4, 4H) ppm. MS (FAB) *m*/*z* (abundance %) = 830 (12) $[M]^+$. Anal. Calcd for $C_{36}H_{61}N_5O_6PdS_2$: C, 52.1; H, 7.4; N, 8.4%. Found: C, 51.9; H, 7.3; N, 8.4%.

Preparation of [Pt(S$_2$C-DO3A-Bu^t)(PPh$_3$)$_2$]PF$_6$ (5). A solution of $[PtCl_2(PPh_3)]_2$ (63 mg, 0.080 mmol) and **1** (50 mg, 0.080 mmol) in chloroform (10 mL) was treated with a solution of NH_4PF_6 (26 mg, 0.159 mmol) in methanol (10 mL) and stirred at room temperature for 16 h. All solvent was removed to give a mixture of white solids, which were dissolved in minimum chloroform and filtered through Celite to give a clear filtrate. The filtrate was concentrated to approximately 1 mL, and then diethyl ether (20 mL) was added to precipitate a white product, which was filtered and dried under vacuum. Yield: 65 mg (56%). IR (solid state): 3048 (ν_{C-H}), 2975, 2928, 2908, 2834 (ν_{C-H}), 1724 ($\nu_{C=O}$), 1503 (ν_{C-N}), 1366 (δ_{C-H}), 1147 (ν_{C-O}), 990 (ν_{C-S}), 848, 740 cm^{-1}. ^1H NMR (400 MHz, CD_2Cl_2): 1.32−1.76 (m, CH_3, 27H), 2.49−4.39 (m, DO3A-^{t}Bu-CS_2 ligand, 22H), 7.27−7.65 (m, C_6H_5, 30H) ppm. ^{31}P NMR (162 MHz, CD_2Cl_2): 14.8 (s, PPh_3, J_{PPt} = 3293 Hz) ppm. MS (FAB) *m*/*z* (abundance %) = 1309 (100) $[M]^+$. Anal. Calcd for $C_{63}H_{79}F_6N_4O_6P_3PtS_2$: C, 52.0; H, 5.5; N, 3.9%. Found: C, 52.2; H, 5.4; N, 3.9%.

Preparation of [Au(S$_2$C-DO3A-Bu^t)(PPh$_3$)] (6). A solution of **1** (50 mg, 0.080 mmol) and $[AuCl(PPh_3)]$ (39 mg, 0.080 mmol) in chloroform (10 mL) was stirred at room temperature for 1 h in the dark. All solvent was removed, and the resultant residue was dissolved in chloroform (3 mL) and filtered through Celite to give a pale yellow solution. All solvent was evaporated to give the product as a pale yellow foamy solid, which was dried under vacuum. Yield: 35 mg (42%). IR (solid state): 3054 (ν_{C-H}), 2975, 2930, 2833 (ν_{C-H}), 1723 ($\nu_{C=O}$), 1479 (ν_{C-N}), 1436, 1366 (δ_{C-H}), 1249, 1218, 1147 (ν_{C-O}), 997 (ν_{C-S}), 968 (ν_{C-S}), 847, 747, 692 cm^{-1}. ^1H NMR (400 MHz, CD_2Cl_2): 1.49 (s, CH_3, 27H), 2.67−2.88 (m, NCH_2, 8H), 3.17 (t, $CH_2CH_2NCS_2$, 4H, J_{HH} = 5.8 Hz), 3.36 (s, CH_2COO^tBu, 6H), 4.29 (t, CH_2NCS_2, 4H, J_{HH} = 5.8 Hz), 7.47−7.60 (m, *o*/*p*-C_6H_5, 9H), 7.60−7.69 (m, *m*-C_6H_5, 6H) ppm. ^{31}P NMR (162 MHz, CD_2Cl_2): 36.1 (s, PPh_3) ppm. MS (FAB) *m*/*z* (abundance %): 1049 (50) $[M]^+$. Anal. Calcd for $C_{45}H_{64}AuN_4PO_6S_2$: C, 51.5; H, 6.2; N, 5.3%. Found: C, 51.7; H, 6.0; N, 5.3%.

Preparation of [Au(S$_2$C-DO3A-Bu^t)(PCy$_3$)] (7). A solution of **1** (50 mg, 0.080 mmol) and $[AuCl(PCy_3)]$ (41 mg, 0.080 mmol) in chloroform (10 mL) was stirred at room temperature for 1 h in the dark. All solvent was removed, and the resultant residue was dissolved in minimum chloroform and filtered through Celite to give a pale yellow solution. All solvent was evaporated to give the product as a pale yellow foamy solid, which was dried under vacuum. Yield: 18 mg (21%). IR (solid state): 2974, 2927, 2851 (ν_{C-H}), 1727 ($\nu_{C=O}$), 1477 (ν_{C-N}), 1366 (δ_{C-H}), 1249, 1217, 1148 (ν_{C-O}), 1001 (ν_{-S}), 970 (ν_{C-S}), 850, 744 cm^{-1}. ^1H NMR (400 MHz, CD_2Cl_2): 1.25−1.47 (m, Cy, 14H), 1.47−1.52 (m, CH_3, 27H), 1.61−2.20 (m, Cy, 19H), 2.69−2.83 (m, NCH_2, 8H), 3.07−3.22 (m, $CH_2CH_2NCS_2$, 4H), 3.30−3.40 (m, CH_2COO^tBu, 6H), 4.25 (t, CH_2NCS_2, 2H, J_{HH} = 5.4 Hz), 4.45 (t, CH_2NCS_2, 2H, J_{HH} = 5.4 Hz) ppm. ^{31}P NMR (162 MHz, CD_2Cl_2): 55.5 (s, PCy_3) ppm. MS (FAB) *m*/*z* (abundance %) = 1067 (4) $[M]^+$. Anal. Calcd for $C_{45}H_{82}AuN_4O_6PS_2{\cdot}0.75CHCl_3$: C, 47.5; H, 7.2; N, 4.8%. Found: C, 47.7; H, 7.0; N, 4.8%.

Preparation of [Au$_2$(S$_2$C-DO3A-Bu^t)$_2$] (8). A solution of **1** (50 mg, 0.080 mmol) and [AuCl(tht)] (26 mg, 0.081 mmol) in chloroform (10 mL) was stirred at room temperature for 1 h. All solvent was removed, and the resultant residue was dissolved in minimum chloroform and filtered through Celite to give a yellow solution. The solution was concentrated, and then pentane (20 mL) was added. All solvent was removed to give a golden yellow foamy solid, which was dried under vacuum. Yield: 37 mg (59%). IR (solid state): 2975, 2931, 2837 (ν_{C-H}), 1724 ($\nu_{C=O}$), 1481 (ν_{C-N}), 1365 (δ_{C-H}), 1146, 1124 (ν_{C-O}), 993 (ν_{C-S}), 847, 744 cm^{-1}. ^1H NMR (400 MHz, CD_2Cl_2): 1.49 (s, CH_3, 18H), 1.50 (s, CH_3, 36H), 2.77 (s, NCH_2, 16H), 3.17 (t, $CH_2CH_2NCS_2$, 8H, J_{HH} = 5.4 Hz), 3.33 (s, CH_2COO^tBu, 4H), 3.35 (s, CH_2COO^tBu, 8H), 4.45 (t, CH_2NCS_2,

dx.doi.org/10.1021/ic401936w | *Inorg. Chem.* 2014, 53, 1989−2005

8H, J_{HH} = 5.4 Hz) ppm. MS (FAB) m/z (abundance %): 1573 (100) $[M]^+$. Anal. Calcd for $C_{54}H_{98}Au_2N_8O_{12}S_4$: C, 41.2; H, 6.3; N, 7.1%. Found: C, 41.1; H, 6.2; N, 7.0%.

Preparation of [Ni(S_2C-DO3A-Bu^t)$_2$] (9). A solution of **1** (300 mg, 0.477 mmol) and $NiCl_2 \cdot 6H_2O$ (57 mg, 0.239 mmol) in methanol (10 mL) was stirred at room temperature for 3 h, during which a green precipitate had formed. All solvent was removed, and the residue was dissolved in a minimum volume of chloroform and filtered through Celite. The solution was concentrated to approximately 2 mL, and methanol (20 mL) was added. The green solid was filtered, washed with methanol (15 mL) and hexane (10 mL), and dried under vacuum. Yield: 206 mg (70%). IR (solid state): 2975, 2936, 2906 (ν_{C-H}), 1723 ($\nu_{C=O}$), 1515 (ν_{C-N}), 1365 (δ_{C-H}), 1214, 1216, 1145, 1129 (ν_{C-O}), 971 (ν_{C-S}), 755 cm^{-1}. ^{1}H NMR (400 MHz, $CDCl_3$): 1.48 (s, CH_3, 18H), 1.49 (s, CH_3, 36H), 2.76 (s, NCH_2, 16H), 3.03 (t, $CH_2CH_2NCS_2$, 8H, J_{HH} = 5.2 Hz), 3.26−3.36 (m, CH_2COO^tBu, 12H), 4.05 (t, $CH_2N(CS_2)CH_2$, 8H, J_{HH} = 5.2 Hz) ppm. ^{13}C NMR (101 MHz, $CDCl_3$): 28.2 (s, CH_3), 49.2 (s, NCH_2), 52.2 (s, NCH_2), 53.6 (s, NCH_2), 54.3 (s, CH_2COO^tBu), 58.4 (s, NCH_2), 81.1 (s, $OC(CH_3)_3$), 170.5 (s, C═O), 170.8 (s, C═O), 205.6 (s, CS_2) ppm. MS (FAB) m/z (abundance %) = 1237 (30) $[M]^+$. Anal. Calcd for $C_{54}H_{98}N_8NiO_{12}S_4$: C, 52.4; H, 8.0; N, 9.1%. Found: C, 52.5; H, 7.9; N, 8.9%.

Preparation of [Cu(S_2C-DO3A-Bu^t)$_2$] (10). Copper(II) chloride (0.32 g, 2.380 mmol) and **1** (3.00 g, 4.770 mmol) formed a suspension in methanol (100 mL), the resulting dark brown reaction mixture was stirred for 3 h at room temperature. All solvent was removed under reduced pressure; the brown residue was dissolved in the minimum amount of chloroform and passed through Celite. The filtrate was concentrated to *ca.* 30 mL, pentane (80 mL) was added and the mixture triturated, after which all solvent was removed under reduced pressure leaving a dark brown solid that was dried under vacuum overnight. Yield: 2.65 g (89%). IR (solid state): 2975, 2932, 2852 (ν_{C-H}), 1720 ($\nu_{C=O}$), 1465 ($\nu_{C=N}$), 1424, 1366 (δ_{C-H}), 1247, 1219 (ν_{C-N}), 1140 (ν_{C-O}), 1046, 972, 936 (ν_{C-S}), 846, 754 cm^{-1}. ^{1}H NMR (400 MHz, $CDCl_3$): 1.48 (m, CH_3, 54H), 2.89 (m, NCH_2, 24H), 3.32 (m, CH_2COO^tBu, 12H), 3.80−4.35 (m, $CH_2N(CS_2)CH_2$, 8H) ppm. ^{13}C NMR (101 MHz, $CDCl_3$): 28.4 (s, CH_3), 28.6 (s,CH_3), 50.9−54.0 (3s, poor signal due to paramagnetism of Cu, likely to be from methylene carbons of the cyclen and/or ^{t}Bu-ester arms), 81.0 (s, $OC(CH_3)_3$), 81.1 (s, $OC(CH_3)_3$), 207.0 (s, CS_2) ppm. MS (ES +ve) m/z (abundance %): 1244 (1) $[M]^+$. Anal. Calcd for $C_{54}H_{100}CuN_8O_{12}S_4$: C, 52.1; H, 8.1; N, 9.0%. Found: C, 52.3; H, 7.9; N, 9.2%.

Preparation of [Co(S_2C-DO3A-Bu^t)$_3$] (11). A solution of **1** (300 mg, 0.477 mmol) and $Co(OAc)_2 \cdot 4H_2O$ (40 mg, 0.159 mmol) in methanol (10 mL) was stirred at room temperature for 2 h. All solvent was removed, and the resultant residue was dissolved in minimum chloroform and filtered through Celite to give a green solution. The solution was concentrated to approximately 3 mL, and then pentane (3 mL) was added. All solvent was then evaporated under reduced pressure to give a dark green foamy solid which was dried under vacuum. Yield: 260 mg (89%). IR (solid state): 2976, 2933, 2839 (ν_{C-H}), 1722 ($\nu_{C=O}$), 1487 (ν_{C-N}), 1365 (δ_{C-H}), 1250, 1218, 1146 (ν_{C-O}), 994 (ν_{C-S}), 847, 747 cm^{-1}. ^{1}H NMR (400 MHz, $CDCl_3$): 1.47 (s, CH_3, 81H), 2.67−2.85 (m, NCH_2, 24H), 3.10 (t, $CH_2CH_2NCS_2$, 12H, J_{HH} = 5.3 Hz), 3.34 (s, CH_2COO^tBu, 18H), 4.05 (t, CH_2NCS_2, 12H, J_{HH} = 5.3 Hz) ppm. ^{13}C NMR (101 MHz, CDC_{l3}): 28.3 (s, CH_3), 47.8 (s, NCH_2), 51.6 (s, NCH_2), 53.2 (s, CH_2COO^tBu), 54.7 (s, NCH_2), 57.9 (s, NCH_2), 80.9 (s, $OCMe_3$), 170.8 (s, C═O), 170.9 (s, C═O), 204.8 (s, CS_2) ppm. MS (FAB) m/z (abundance %) = 1828 (55) $[M]^+$. Anal. Calcd for $C_{81}H_{147}CoN_{12}O_{18}S_6$: C, 53.2; H, 8.1; N, 9.2%. Found: C, 53.3; H, 8.0; N, 9.1%.

Preparation of [Ni(S_2C-DO3A)$_2$] (12). A solution of **9** (206 mg, 0.166 mmol) in dichloromethane (12 mL) was treated with trifluoroacetic acid (4 mL) and stirred at room temperature for 50 h. All solvent was removed, and the residue was triturated in dichloromethane (10 mL) followed by evaporation of the dichloromethane. This process was repeated two more times. The previous steps were repeated using methanol (3 × 10 mL) to ensure as much trifluoroacetic acid was removed as possible. The residue was dissolved in methanol (5 mL), and then diethyl ether (10 mL) was added to precipitate the pale green product, which was washed with diethyl ether (15 mL), water (15 mL), ethanol (15 mL), and then pentane (15 mL), and dried under vacuum. Yield: 147 mg (98%). IR (solid state): 3401 (ν_{O-H}), 2954 (ν_{C-H}), 2846, 2528, 1945, 1715 ($\nu_{C=O}$), 1616, 1499 (ν_{C-N}), 1424, 1366, 1215 (ν_{C-O}), 1133, 1086, 968 (ν_{C-S}), 880, 793, 686 cm^{-1}. ^{1}H NMR (400 MHz, DMSO-d^6): 2.76−3.14 (m, NCH_2, 6H), 3.42 (s(br), CH_2COOH, 12H), 3.91 (s(br), NCH_2, 26H) ppm. MS (FAB) m/z (abundance %) = 901 (1) $[M]^+$. Anal. Calcd for $C_{30}H_{50}N_8NiO_{12}S_4$: C, 40.0; H, 5.6; N, 12.4%. Found: C, 40.2; H, 5.5; N, 12.3%.

Preparation of [Cu(S_2C-DO3A)$_2$] (13). A dark brown dichloromethane (140 mL) solution of **10** (2.30 g, 1.847 mmol) was treated with trifluoroacetic acid (46 mL) and stirred at room temperature for *ca.* 60 h. All solvent was then removed under reduced pressure, and the resultant viscous green residue was triturated in dichloromethane (150 mL), followed by evaporation of the solvent as a means to remove any remaining trifluoroacetic acid. This process was repeated twice more with dichloromethane and a further three times using methanol (100 mL). Finally, the resulting residue was dissolved in the minimum amount of methanol, and excess diethyl ether (250 mL) was added to precipitate out the product as a brown solid that was collected by filtration. The product was washed with cold diethyl ether (3 × 40 mL), cold ethanol (3 × 40 mL), and cold pentane (3 × 30 mL), and then dried under vacuum overnight. Yield: 1.68 g (quantitative). IR (solid state): 2865 (ν_{C-H}), 1708 ($\nu_{C=O}$), 1635 (asym-ν_{O-C-O}), 1490 ($\nu_{C=N}$), 1410 (δ_{C-H}), 1250 (ν_{C-C}), 1184 (ν_{C-N}), 1133 (ν_{C-O}), 1087, 985 (ν_{C-S}), 888, 798, 685 cm^{-1}. ^{1}H NMR (400 MHz, D_2O): 2.75−3.30 (m, NCH_2, 24H), 3.80 (s, CH_2COOH, 12H), 3.91 (s, NCH_2, 8H) ppm. MS (ES +ve) m/z (abundance %): 485 (9) [M − DO3A-CS_2]$^+$, 906 (11) $[M]^+$. Anal. Calcd for $C_{30}H_{52}CuN_8O_{12}S_4$: C, 39.7; H, 5.8; N, 12.3%. Found: C, 39.7; H, 5.5; N, 12.41%.

Preparation of [Co(S_2C-DO3A)$_3$] (14). A solution of **11** (100 mg, 0.055 mmol) in dichloromethane (6 mL) was treated with trifluoroacetic acid (2 mL) and stirred at room temperature for 45 h. All solvent was removed, and the residue was triturated in dichloromethane (10 mL) followed by evaporation of the dichloromethane. This process was repeated two more times. The previous steps were repeated using methanol (3 × 10 mL) to ensure as much trifluoroacetic acid was removed as possible. The residue was dissolved in methanol (2 mL), and then the green product was precipitated by careful addition of diethyl ether (10 mL). The green solid was filtered, washed with diethyl ether (15 mL), ethanol (15 mL), and then pentane (15 mL), and dried under vacuum. Yield: 64 mg (88%). IR (solid state): 3409 (ν_{O-H}), 2856 (ν_{C-H}), 2538, 1719 ($\nu_{C=O}$), 1621, 1485 (ν_{C-N}), 1416, 1390, 1357, 1219 (ν_{C-O}), 1189, 1132 (ν_{C-N}), 1084, 966 (ν_{C-S}), 882, 685 cm^{-1}. ^{1}H NMR (400 MHz, D_2O): 2.97−3.56 (m, NCH_2, 36H), 3.67 (s(br), CH_2COOH, 18H), 4.04 (s(br), NCH_2, 12H) ppm. MS (MALDI) m/z (abundance %) = 1325 (93) $[M + 2H]^+$. Anal. Calcd for $C_{45}H_{75}CoN_{12}O_{18}S_6$: C, 40.8; H, 5.7; N, 12.7%. Found: C, 40.6; H, 5.6; N, 12.6%.

Preparation of [Ni(S_2C-DO3A-Gd)$_2$] (15). (a) A suspension of **12** (30 mg, 0.033 mmol) and $GdCl_3$ (25 mg, 0.066 mmol) in an acetate buffer solution (pH 5.5, 10 mL) was stirred at room temperature for 24 h. All solvent was removed and the solid redissolved in water (adjusted to pH 9) and filtered through Celite. The solvent was then removed, and the turquoise crystalline product was then dried under vacuum. Yield: 20 mg (50%). (b) A suspension of **12** (60 mg, 0.0665 mmol) in methanol (50 mL) was treated with $Gd(OTf)_3$ (81 mg, 0.134 mmol) and stirred at room temperature for 24 h. All solvent was removed and the solid redissolved in methanol and triturated with diethyl ether (10 mL), filtered and washed further with diethyl ether (10 mL). The product was then dried under vacuum. Yield: 43 mg (53%). IR (solid state): 3358 (ν_{O-H}), 2950, 2885, 2265, 1731 (asym-ν_{O-C-O}), 1594 (asym-ν_{O-C-O}), 1490 (ν_{C-N}), 1414 (sym-ν_{O-C-O}), 1254 (sym-ν_{O-C-O}), 1224, 1155 (ν_{C-N}), 1089, 1026, 980 (ν_{C-S}), 827, 719, 633 cm^{-1}. MS (FAB) m/z (abundance %) = 1212 (2) $[M]^+$. Anal.

dx.doi.org/10.1021/ic401936w | *Inorg. Chem.* 2014, 53, 1989−2005

Calcd for $C_{30}H_{46}Gd_2N_8NiO_{12}S_4$: C, 29.7; H, 3.8; N, 9.2%. Found: C, 29.4; H, 3.9; N, 9.0%.

Preparation of [Cu(S$_2$C-DO3A-Gd)$_2$] (16). To a solution of **13** (1.40 g, 1.541 mmol) in water (300 mL) was added a solution of gadolinium(III) triflate (1.86 g, 3.077 mmol) in water (50 mL). The brown reaction mixture was stirred for 24 h at room temperature. All solvent was removed under reduced pressure and the residue dissolved in the minimum amount of water, excess ethanol (200 mL) was added, and the suspension was triturated. The dark brown product was collected by filtration, washed with cold ethanol (3 × 30 mL), and dried under vacuum overnight. Yield: 1.46 g (78%). IR (solid state): 3325 (ν_{O-H}), 1591 (asym-ν_{O-C-O}), 1460 (sym-ν_{O-C-O}), 1412 (δ_{C-H}), 1246, 1225 (sym-ν_{O-C-O}), 1165, 1120 (ν_{C-N}), 1026 (ν_{C-S}), 635 cm^{-1}. MS (ES +ve) *m*/*z* (abundance %): 1217 (1) [M]$^+$. Anal. Calcd for $C_{30}H_{46}CuGd_2N_8O_{12}S_4$: C, 29.6; H, 3.8; N, 9.2%. Found: C, 30.2; H, 3.7; N, 9.2%.

Preparation of [Co(S$_2$C-DO3A-Gd)$_3$] (17). A solution of **14** (25 mg, 0.019 mmol) in water (15 mL) was treated with a solution of Gd(OTf)$_3$ (34 mg, 0.057 mmol) in water (3 mL) and stirred at room temperature for 24 h leading to a suspension. The solvent was removed under reduced pressure and the residue then dissolved in methanol (3 mL). Ethanol (20 mL) was added to precipitate the dark green product, which was washed with cold ethanol (25 mL) and diethyl ether (20 mL) and dried under vacuum. Yield: 22 mg (65%). IR (solid state): 3393 (ν_{O-H}), 2851 (ν_{C-H}), 1559 (asym-ν_{O-C-O}), 1488 (ν_{C-N}), 1413 (sym-ν_{O-C-O}), 1238 (sym-ν_{O-C-O}), 1225, 1163 (ν_{C-N}), 1088, 1027 (ν_{C-S}), 726, 635 cm^{-1}. MS (FAB) *m*/*z* (abundance %) = 1787 (5) [M]$^+$. Anal. Calcd for $C_{45}H_{66}CoGd_3N_{12}O_{18}S_6{\cdot}H_2O$: C, 30.3; H, 3.7; N, 9.4%. Found: C, 30.2; H, 3.7; N, 9.4%.

Preparation of [Co(S$_2$C-DO3A-La)$_3$] (18). A solution of **14** (25 mg, 0.019 mmol) in water (15 mL) was treated with $LaCl_3{\cdot}7H_2O$ (22 mg, 0.058 mmol) and stirred at room temperature for 24 h. The solvent was then evaporated to give a green residue which was triturated in methanol (10 mL) to give a fine dark green solid. The dark green product was filtered and washed with methanol (20 mL) and pentane (20 mL) and dried under vacuum. Yield: 30 mg (92%). IR (solid state): 3303 (ν_{O-H}), 2991, 2851, 2588, 1724 (asym-ν_{O-C-O}), 1600 (asym-ν_{O-C-O}), 1483 (ν_{C-N}), 1405 (sym-ν_{O-C-O}), 1337, 1235 (sym-ν_{O-C-O}), 1188 (ν_{C-N}), 1144, 1087, 1017, 967 (ν_{C-S}), 933 cm^{-1}. ^{1}H NMR (400 MHz, D_2O): 3.16−3.39 (m, NCH_2, 24H), 3.49 (s(br), $CH_2CH_2NCS_2$, 12H), 3.68 (m, CH_2COO, 18H), 4.08 (s, CH_2NCS_2, 12H) ppm. MS (FAB) *m*/*z* (abundance %) not diagnostic. Anal. Calcd for $C_{45}H_{66}CoLa_3N_{12}O_{18}S_6$: C, 31.2; H, 3.8; N, 9.7%. Found: C, 31.0; H, 3.5; N, 9.6%.

Preparation of Au@S$_2$C-DO3A-^{t}Bu (NP1). A solution of $HAuCl_4$ (198 mg, 0.58 mmol) in distilled water (600 mL) was heated at reflux with vigorous stirring. Trisodium citrate (602 mg, 2.33 mmol) in distilled water (50 mL) was added, and heating continued for 10 min. The reaction was stirred for a further 15 min at room temperature. A solution of **1** (1.10 g, 1.75 mmol) in distilled water (20 mL) was added dropwise over 10 min, causing precipitation of a fine solid. The reaction was allowed to stir for a further 3 h, and then stored overnight at 6 °C. The brown precipitate was collected by centrifuging, washed thoroughly with water (5 × 10 mL), and dried under vacuum. IR (solid state): 2976, 2930, 2848 (ν_{C-H}), 1722 ($\nu_{C=O}$), 1455 (ν_{C-N}), 1366 (δ_{C-H}), 1249, 1217, 1146 (ν_{C-O}), 969 (ν_{C-S}), 937 (ν_{C-S}), 847, 747 cm^{-1}. ^{1}H NMR (400 MHz, $CDCl_3$): 1.45, 1.46, 1.47 (s × 3, *tert*-Bu, 27H), 2.74−2.84 (m, NCH_2, 8H), 3.10 (m, NCH_2, 4H), 3.18 (t, CH_2NCS_2, 2H, J_{HH} = 5.9 Hz), 3.33−3.40 (m, CH_2CO_2, 6H), 4.42 (t, CH_2NCS_2, 2H, J_{HH} = 5.9 Hz) ppm. TEM analysis of 100 nanoparticles gave a size of 19.7 ± 3.7 nm. EDS indicated the presence of gold and sulfur.

Preparation of Au@S$_2$C-DO3A-^{t}Bu (NP2). A solution of $HAuCl_4$ (270 mg, 0.79 mmol) in methanol (60 mL) was treated with a solution of **1** (500 mg, 0.79 mmol) in water (40 mL) with vigorous stirring. The solution was cooled to 4 °C and stirred for 10 min. A freshly prepared aqueous solution (10 mL) of sodium borohydride (252 mg, 6.66 mmol) was added dropwise over 20 min, with the temperature maintained at 4 °C. A color change from orange to dark brown was observed upon addition of the reducing agent. The reaction was stirred for 3 h at 10 °C. The brown precipitate was collected by centrifuging, washed thoroughly with water (5 × 10 mL), and dried under vacuum. IR (solid state): 2974, 2930, 2841 (ν_{C-H}), 1722 ($\nu_{C=O}$), 1460 (ν_{C-N}), 1410, 1363 (δ_{C-H}), 1135 (ν_{C-O}), 993 (ν_{C-S}), 945 (ν_{C-S}), 845, 749 cm^{-1}. ^{1}H NMR (400 MHz, $CDCl_3$): 1.48, 1.49 (s × 2, *tert*-Bu, 27H), 2.77−2.84 (m, NCH_2, 8H), 2.95 (m, NCH_2, 4H), 3.18 (t, CH_2NCS_2, 2H, J_{HH} = 5.0 Hz), 3.35−3.38 (m, CH_2CO_2, 6H), 4.42 (t, CH_2NCS_2, 2H, J_{HH} = 5.0 Hz) ppm. TEM analysis of 100 nanoparticles gave a size of 3.7 ± 1.0 nm. EDS indicated the presence of gold and sulfur.

Preparation of Au@S$_2$C-DO3A (NP3). Trifluoroacetic acid (0.2 mL) was added to a solution of **NP1** (50 mg) in chloroform (10 mL), and the reaction was stirred for 60 h. All solvents were removed, and the dark brown product was washed with chloroform (3 × 5 mL) and cold ethanol (3 × 5 mL) to remove the acid. The product was dissolved in a minimum volume of methanol and precipitated with diethyl ether. Centrifuging was employed to collect the dark brown product, and the nanoparticles were dried under vacuum. IR (solid state): 2432, 1739 ($\nu_{C=O}$), 1450 (ν_{C-N}), 1410, 1364 (δ_{C-H}), 1218 (ν_{C-O}), 1101, 920 (ν_{C-S}) cm^{-1}. ^{1}H NMR (400 MHz, D_2O): 2.76−3.15 (m, NCH_2, 12H), 3.23 (m, CH_2NCS_2, 2H), 3.34−3.38 (m, CH_2CO_2, 6H), 3.53−3.57 (m, CH_2NCS_2, 2H) ppm. TEM analysis of 100 nanoparticles gave a size of 18.9 ± 4.8 nm. EDS indicated the presence of gold and sulfur.

Preparation of Au@S$_2$C-DO3A (NP4). Trifluoroacetic acid (0.2 mL) was added to a solution of **NP2** (50 mg) in chloroform (10 mL) and the reaction stirred for 72 h. All solvent was removed, and the dark brown product was washed with chloroform (3 × 5 mL) and cold ethanol (3 × 5 mL). The product was dissolved in a minimum volume of methanol and precipitated with diethyl ether. Centrifuging was employed to collect the dark brown product, and the nanoparticles were dried under vacuum. IR (solid state): 3368 (ν_{O-H}), 2975, 2932 (ν_{C-H}), 1721 ($\nu_{C=O}$), 1680 ($\nu_{C=O}$), 1461 (ν_{C-N}), 1391, 1364 (δ_{C-H}), 1231, 1197, 1146 (ν_{C-O}), 992 (ν_{C-S}), 945 (ν_{C-S}), 833 cm^{-1}. ^{1}H NMR (400 MHz, $CDCl_3$): 2.77−2.94 (m, NCH_2, 12H), 3.11 (m, CH_2NCS_2, 2H), 3.28−3.34 (m, CH_2CO_2, 6H), 4.37 (m, CH_2NCS_2, 2H) ppm. TEM analysis of 100 nanoparticles gave a size of 3.7 ± 0.9 nm. EDS indicated the presence of gold and sulfur.

Preparation of Au@S$_2$C-DO3A-Gd (NP5). (a) A suspension of **NP3** (10 mg) was stirred overnight at room temperature in a 5 mM solution of $GdCl_3$ (acetate buffer, pH 5.5). After removing the supernatant aqueous solution, the nanoparticles were washed with water (5 × 10 mL) and then isolated by centrifuging. The black product was dried overnight under vacuum. (b) **NP3** (30 mg) was dissolved in methanol (10 mL) and treated with a methanolic solution (5 mL) of Gd(OSO$_2$CF$_3$)$_3$ (30 mg, 0.05 mmol). The mixture was stirred for 24 h at room temperature. The solvent was then removed to produce a black product, which was dissolved in a minimum volume of methanol and precipitated with diethyl ether. The product was isolated by centrifuging and the nanoparticles washed with water (10 × 5 mL). The dark brown product was dried overnight under vacuum. IR (solid state): 3387 (ν_{O-H}), 2895 (ν_{C-H}), 1717 ($\nu_{C=O}$), 1605 ($\nu_{C=O}$), 1466 (ν_{C-N}), 1362 (δ_{C-H}), 1232 (ν_{C-O}), 1145 (ν_{C-O}), 1029, 960 (ν_{C-S}), 841 cm^{-1}. TEM analysis of 100 nanoparticles gave a size of 18.6 ± 4.3 nm. EDS indicated the presence of gold, sulfur, and gadolinium.

Relaxation Experiments. Gd(III) compounds were prepared *in situ* by mixing the appropriate amounts of ligand and Gd(III) salt (99.99%; Aldrich) in H_2O followed by adjustment of the pH with NaOH aqueous solution (pH = 7.4). The resulting solution was placed in a 1.7 mm diameter capillary which was sealed. The absence of free gadolinium was determined in all samples by the xylenol orange test. The $1/T_1$ measurements were performed on a Bruker Avance DRX400 spectrometer (400 MHz). Gadolinium content in the range of 312 complexes per gold nanoparticle was determined for independent syntheses by combined magnetic susceptibility measurements and TEM measurements.[64]

Crystallography. Table 1 provides a summary of the crystallographic data for compound **9**. Data were collected using an Oxford Diffraction Xcalibur 3 diffractometer, and the structure was refined

dx.doi.org/10.1021/ic401936w | *Inorg. Chem.* 2014, 53, 1989−2005

Table 1. Crystallographic Data for Compound 9

data	9
chemical formula	$C_{54}H_{98}N_8NiO_{12}S_4$
solvent	none
fw	1238.35
T (°C)	−100
space group	$P\bar{1}$ (No. 2)
a (Å)	11.2673(5)
b (Å)	12.2807(5)
c (Å)	13.3887(4)
α (deg)	111.889(3)
β (deg)	94.522(3)
γ (deg)	104.051(3)
V (Å^3)	1637.83(12)
Z	1[a]
ρ_{calcd} (g cm^{-3})	1.256
λ (Å)	0.71073
μ (mm^{-1})	0.484
R1 (obsd)[b]	0.0465
wR2 (all)[c]	0.1323

[a]The molecule has crystallographic C_i symmetry. [b]$R1 = \Sigma||F_o| - |F_c||/\Sigma|F_o|$. [c]$wR2 = \{\Sigma[w(F_o^2 - F_c^2)^2]/\Sigma[w(F_o^2)^2]\}^{1/2}$; $w^{-1} = \sigma^2(F_o^2) + (aP)^2 + bP$.

based on F^2 using the SHELXTL and SHELX-97 program systems.[73] CCDC 930886 contains the relevant data.

■ ASSOCIATED CONTENT

Supporting Information

Additional experimental details and figures. CIF file with crystallographic data for the structure of **9**. This material is available free of charge via the Internet at http://pubs.acs.org.

■ AUTHOR INFORMATION

Corresponding Author

*E-mail: j.wilton-ely@imperial.ac.uk.

Notes

The authors declare no competing financial interest.

■ ACKNOWLEDGMENTS

We thank Dr. Simon J. A. Pope for helpful discussions at the inception of this project. Prof. Nicholas J. Long is acknowledged for the generous provision of characterization facilities. We gratefully acknowledge the support of the Leverhulme Trust (Grant RPG-2012-634) for a studentship (A.T.). We are grateful to Johnson Matthey Ltd. for a generous loan of ruthenium and gold salts.

■ REFERENCES

(1) (a) Amijs, C. H. M.; van Clink, G. P. M.; van Koten, G. *Dalton Trans.* **2006**, 308−327. (b) Janiak, C. *Dalton Trans.* **2003**, 2781−2804. (c) Arora, H.; Mukherjee, R. *New J. Chem.* **2010**, *34*, 2357−2365.

(2) (a) Li, H.; Eddaoudi, M.; O'Keeffe, M.; Yaghi, O. *Nature* **1999**, *402*, 276−279. (b) Long, J. R.; Yaghi, O. M. *Chem. Soc. Rev.* **2009**, *38*, 1213−1214 and subsequent reviews in the same issue. (c) Janiak, C.; Vieth, J. K. *New J. Chem.* **2010**, *34*, 2366−2388.

(3) (a) Wilton-Ely, J. D. E. T.; Solanki, D.; Hogarth, G. *Eur. J. Inorg. Chem.* **2005**, 4027−4030. (b) Knight, E. R.; Solanki, D.; Hogarth, G.; Holt, K. B.; Thompson, A. L.; Wilton-Ely, J. D. E. T. *Inorg. Chem.* **2008**, *47*, 9642−9653. (c) Macgregor, M. J.; Hogarth, G.; Thompson, A. L.; Wilton-Ely, J. D. E. T. *Organometallics* **2009**, *28*, 197−208. (d) Naeem, S.; Ogilvie, E.; White, A. J. P.; Hogarth, G.; Wilton-Ely, J. D. E. T. *Dalton Trans.* **2010**, *39*, 4080−4089. (e) Naeem, S.; White, A. J. P.; Hogarth, G.; Wilton-Ely, J. D. E. T. *Organometallics* **2010**, *29*, 2547−2556. (f) Oliver, K.; Hogarth, G.; White, A. J. P.; Wilton-Ely, J. D. E. T. *Dalton Trans.* **2011**, *40*, 5852−5864. (g) Lin, Y. H.; Leung, N. H.; Holt, K. B.; Thompson, A. L.; Wilton-Ely, J. D. E. T. *Dalton Trans.* **2009**, 7891−7901.

(4) (a) Knight, E. R.; Cowley, A. R.; Hogarth, G.; Wilton-Ely, J. D. E. T. *Dalton Trans.* **2009**, 607−609. (b) Knight, E. R.; Leung, N. H.; Lin, Y. H.; Cowley, A. R.; Watkin, D. J.; Thompson, A. L.; Hogarth, G.; Wilton-Ely, J. D. E. T. *Dalton Trans.* **2009**, 3688−3697. (c) Knight, E. R.; Leung, N. H.; Thompson, A. L.; Hogarth, G.; Wilton-Ely, J. D. E. T. *Inorg. Chem.* **2009**, *48*, 3866−3874.

(5) Carr, D.; Brown, J.; Bydder, G.; Steiner, R.; Weinmann, H.; Speck, U.; Hall, A.; Young, I. *AJR, Am. J. Roentgenol.* **1984**, *143*, 215−224.

(6) Cacheris, W. P.; Quay, S. C.; Rocklage, S. M. *Magn. Reson. Imaging* **1990**, *8*, 467−481.

(7) Idée, J.-M.; Port, M.; Robic, C.; Medina, C.; Sabatou, M.; Corot, C. *J. Magn. Reson. Imaging* **2009**, *30*, 1249−1258.

(8) Ranganathan, R. S.; Raju, N.; Fan, H.; Zhang, X.; Tweedle, M. F.; Desreux, J. F.; Jacques, V. *Inorg. Chem.* **2002**, *41*, 6856−6866.

(9) Caravan, P. *Chem. Soc. Rev.* **2006**, *35*, 512−523.

(10) Cavanagh, J. *Protein NMR Spectroscopy: Principles and Practice*; Academic Press: New York, 2007.

(11) Rohrer, M.; Bauer, H.; Mintorovitch, J.; Requardt, M.; Weinmann, H.-J. *Invest. Radiol.* **2005**, *40*, 715−724.

(12) (a) Nicolle, G. M.; Tóth, E.; Schmitt-Willich, H.; Radüchel, B.; Merbach, A. E. *Chem.—Eur. J.* **2002**, *8*, 1040−1048. (b) Laus, S.; Sour, A.; Ruloff, R.; Tóth, E.; Merbach, A. E. *Chem.—Eur. J.* **2005**, *11*, 3064−3076.

(13) Tóth, E.; Helm, L.; Kellar, K. E.; Merbach, A. E. *Chem.—Eur. J.* **1999**, *5*, 1202−1211.

(14) Dunand, F. A.; Tóth, E.; Hollister, R.; Merbach, A. E. *JBIC, J. Biol. Inorg. Chem.* **2001**, *6*, 247−255.

(15) (a) Dehaen, G.; Verwilst, P.; Eliseeva, S. V.; Laurent, S.; Vander Elst, L.; Muller, R. N.; De Borggraeve, W. M.; Binnemans, K.; Parac-Vogt, T. N. *Inorg. Chem.* **2011**, *50*, 10005−10014. (b) Dehaen, G.; Eliseeva, S. V.; Kimpe, K.; Laurent, S.; Vander Elst, L.; Muller, R. N.; Dehaen, W.; Binnemans, K.; Parac-Vogt, T. N. *Chem.—Eur. J.* **2012**, *18*, 293−302. (c) Debroye, E.; Dehaen, G.; Eliseeva, S. V.; Laurent, S.; Vander Elst, L.; Muller, R. N.; Binnemansa, K.; Parac-Vogt, T. N. *Dalton Trans.* **2012**, *41*, 10549−10556. (d) Verwilst, P.; Eliseeva, S. V.; Vander Elst, L.; Burtea, C.; Laurent, S.; Petoud, S.; Muller, R. N.; Parac-Vogt, T. N.; De Borggraeve, W. M. *Inorg. Chem.* **2012**, *51*, 6405−6411. (e) Dehaen, G.; Eliseeva, S. V.; Verwilst, P.; Laurent, S.; Vander Elst, L.; Muller, R. N.; De Borggraeve, W.; Binnemans, K.; Parac-Vogt, T. N. *Inorg. Chem.* **2012**, *51*, 8775−8783.

(16) (a) Livramento, J. B.; Tóth, E.; Sour, A.; Borel, A.; Merbach, A. E.; Ruloff, R. *Angew. Chem., Int. Ed.* **2005**, *44*, 1480−1484. (b) Livramento, J. B.; Sour, A.; Borel, A.; Merbach, A. E.; Tóth, E. *Chem.—Eur. J.* **2006**, *12*, 989−1003.

(17) Bryant, L. H.; Brechbiel, M. W.; Wu, C.; Bulte, J. W. M.; Herynek, V.; Frank, J. A. *J. Magn. Reson. Imaging* **1999**, *9*, 348−352.

(18) Livramento, J. B.; Weidensteiner, C.; Prata, M. I. M.; Allegrini, P. R.; Geraldes, C. F. G. C.; Helm, L.; Kneuer, R.; Merbach, A. E.; Santos, A. C.; Schmidt, P.; Tóth, E. *Contrast Media Mol. Imaging* **2006**, *1*, 30−39.

(19) Costa, J.; Ruloff, R.; Burai, L.; Helm, L.; Merbach, A. E. *J. Am. Chem. Soc.* **2005**, *127*, 5147−5157.

(20) Moriggi, L.; Aebischer, A.; Cannizzo, C.; Sour, A.; Borel, A.; Bunzli, J.-C. G.; Helm, L. *Dalton Trans.* **2009**, 2088−2095.

(21) Comblin, V.; Gilsoul, D.; Hermann, M.; Humblet, V.; Jacques, V.; Mesbahi, M.; Sauvage, C.; Desreux, J. F. *Coord. Chem. Rev.* **1999**, *185−186*, 451−470.

(22) Powell, D. H.; Dhubhghaill, O. M. N.; Pubanz, D.; Helm, L.; Lebedev, Y. S.; Schlaepfer, W.; Merbach, A. E. *J. Am. Chem. Soc.* **1996**, *118*, 9333−9346.

(23) (a) Tóth, E.; Vauthey, S.; Pubanz, D.; Merbach, A. E. *Inorg. Chem.* **1996**, *35*, 3375−3379. (b) Costa, J.; Balogh, E.; Turcry, V.; Tripier, R.; Le Baccon, M.; Chuburu, F.; Handel, H.; Helm, L.; Tóth,

E.; Merbach, A. E. *Chem.—Eur. J.* **2006**, *12*, 6841−6851. (c) Livramento, J. B.; Helm, L.; Sour, A.; O'Neil, C.; Merbach, A. E.; Tóth, E. *Dalton Trans.* **2008**, 1195−1202.
(24) Mieville, P.; Jaccard, H.; Reviriego, F.; Tripier, R.; Helm, L. *Dalton Trans.* **2011**, *40*, 4260−4267.
(25) (a) Coucouvanis, D. *Prog. Inorg. Chem.* **1970**, *11*, 233−371. (b) Coucouvanis, D. *Prog. Inorg. Chem.* **1979**, *26*, 301−469. (c) Hogarth, G. *Prog. Inorg. Chem.* **2005**, *53*, 71−561.
(26) Supkowski, R. M.; Horrocks, W. D. *Inorg. Chem.* **1999**, *38*, 5616−5619.
(27) (a) Boisselier, E.; Astruc, D. *Chem. Soc. Rev.* **2009**, *38*, 1759−1782. (b) For a recent example, see: Liang, G.; Ye, D.; Zhang, X.; Dong, F.; Chen, H.; Zhang, S.; Li, J.; Shenc, X.; Kong, J. *J. Mater. Chem. B* **2013**, *1*, 3545−3618.
(28) Jun, Y.; Lee, J.-H.; Cheon, J. *Angew. Chem., Int. Ed.* **2008**, *47*, 5122−5135.
(29) Moriggi, L.; Cannizzo, C.; Dumas, E.; Mayer, C. R.; Ulianov, A.; Helm, L. *J. Am. Chem. Soc.* **2009**, *131*, 10829−10829.
(30) Stasiuk, G. J.; Tamang, S.; Imbert, D.; Poillot, C.; Giardiello, M.; Tisseyre, C.; Barbier, E. L.; Fries, P. H.; de Waard, M.; Reiss, P.; Mazzanti, M. *ACS Nano* **2011**, *5*, 8193−8201.
(31) Leff, D. V.; Brandt, L.; Heath, J. R. *Langmuir* **1996**, *12*, 4723−4730.
(32) Schmid, G. *Clusters and Colloids: From Theory to Applications*; VCH: Wiley: New York, 1994.
(33) Jennings, L. E.; Long, N. J. *Chem. Commun.* **2009**, 3511−3524.
(34) Alric, C.; Taleb, J.; Duc, G. L.; Mandon, C.; Billotey, C.; Meur-Herland, A. L.; Brochard, T.; Vocanson, F.; Janier, M.; Perriat, P.; Roux, S.; Tillement, O. *J. Am. Chem. Soc.* **2008**, *130*, 5908−5915.
(35) Debouttière, P. J.; Roux, S.; Vocanson, F.; Billotey, C.; Beuf, O.; Favre-Réguillon, A.; Lin, Y.; Pellet-Rostaing, S.; Lamartine, R.; Perriat, P.; Tillement, O. *Adv. Funct. Mater.* **2006**, *16*, 2330−2339.
(36) Park, J.-A.; Reddy, P. A. N.; Kim, H.-K.; Kim, I.-S.; Kim, G.-C.; Chang, Y.; Kim, T.-J. *Bioorg. Med. Chem. Lett.* **2008**, *18*, 6135−6137.
(37) Marradi, M.; Alcántara, D.; de la Fuente, J. M.; García-Martín, M. L.; Cerdán, S.; Penadés, S. *Chem. Commun.* **2009**, 3922−3924.
(38) Warsi, M. F.; Adams, R. W.; Duckett, S. B.; Chechik, V. *Chem. Commun.* **2010**, *46*, 451−453.
(39) Warsi, M. F.; Chechik, V. *Phys. Chem. Chem. Phys.* **2011**, *13*, 9812−9817.
(40) (a) Loo, C.; Lowery, A.; Halas, N.; West, J.; Drezek, R. *Nano Lett.* **2005**, *5*, 709−711. (b) Huang, X.; El-Sayed, I. H.; Qian, W.; El-Sayed, M. A. *J. Am. Chem. Soc.* **2006**, *128*, 2115−2120.
(41) Lim, Y. T.; Cho, M. Y.; Choi, B. S.; Lee, J. M.; Chung, B. H. *Chem. Commun.* **2008**, 4930−4932.
(42) Daniel, M.-C.; Astruc, D. *Chem. Rev.* **2003**, *104*, 293−346.
(43) (a) Zhao, Y.; Pérez-Segarra, W.; Shi, Q.; Wei, A. *J. Am. Chem. Soc.* **2005**, *127*, 7328−7329. (b) Cormode, D. P.; Davis, J. J.; Beer, P. D. *J. Inorg. Organomet. Polym.* **2008**, *18*, 32−40. (c) Hansen, M. N.; Chang, L.-S.; Wei, A. *Supramol. Chem.* **2008**, *20*, 35−40.
(44) Naeem, S.; Serapian, S.; Toscani, A.; White, A. J. P.; Hogarth, G.; Wilton-Ely, J. D. E. T. DOI: 10.1021/ic402048a.
(45) Stasiuk, G.; Long, N. J. *Chem. Commun.* **2013**, *49*, 2732−2746.
(46) Jagadish, B.; Brickert-Albrecht, G. L.; Nichol, G. S.; Mash, E. A.; Raghunand, N. *Tetrahedron Lett.* **2011**, *52*, 2058−2061.
(47) Paris, J.; Gameiro, C.; Humblet, V.; Mohapatra, P. K.; Jacques, V.; Desreux, J. F. *Inorg. Chem.* **2006**, *45*, 5092−5102.
(48) (a) Humeres, E.; Debacher, N. A.; Franco, J. D.; Lee, B. S.; Martendal, A. *J. Org. Chem.* **2002**, *67*, 3662−3667. (b) Humeres, E.; Debacher, N. A.; Sierra, M. M. de S.; Franco, J. D.; Schutz, A. *J. Org. Chem.* **1998**, *63*, 1598−1603. (c) Humeres, E.; Debacher, N. A.; Sierra, M. M. de S. *J. Org. Chem.* **1999**, *64*, 1807−1813. (d) Ewing, S. P.; Lockshon, D.; Jencks, W. P. *J. Am. Chem. Soc.* **1980**, *102*, 3072−3084.
(49) Delépine, M. *Compt. Rend.* **1907**, *144*, 1125.
(50) Granell, J.; Green, M. L. H.; Lowe, V. J.; Marder, S. R.; Mountford, P.; Saunders, G. C.; Walker, N. M. *J. Chem. Soc., Dalton Trans.* **1990**, 605−614.
(51) Allen, F. H.; Kennard, O.; Watson, D. G.; Brammer, L.; Orpen, A. G.; Taylor, R. *J. Chem. Soc., Perkin Trans. 2* **1987**, S1−S19.
(52) Kobayashi, S.; Anwander, R. *Lanthanides: Chemistry and Use in Organic Synthesis*; Springer: New York, 1999.
(53) Pierre, V. C.; Botta, M.; Aime, S.; Raymond, K. N. *Inorg. Chem.* **2006**, *45*, 8355−8364.
(54) Sinclair, R. G.; McKay, A. F.; Myers, G. S.; Jones, R. N. *J. Am. Chem. Soc.* **1952**, *74*, 2578−2585.
(55) Nonat, A.; Fries, P. H.; Pecaut, J.; Mazzanti, M. *Chem.—Eur. J.* **2007**, *13*, 8489−8506.
(56) Gardiello, M.; Lowe, M. P.; Botta, M. *Chem. Commun.* **2007**, *39*, 4044−4046.
(57) (a) Wessels, J. M.; Nothofer, H.-G.; Ford, W. E.; von Wrochem, F.; Scholz, F.; Vossmeyer, T.; Schroedter, A.; Weller, H.; Yasuda, A. *J. Am. Chem. Soc.* **2004**, *126*, 3349−3356. (c) Vickers, M. S.; Cookson, J.; Beer, P. D.; Bishop, P. T.; Thiebaut, B. *J. Mater. Chem.* **2006**, *16*, 209−215. (d) Sharma, J.; Chhabra, R.; Yan, H.; Liu, Y. *Chem. Commun.* **2008**, 2140−2142. (e) Zhu, H.; Coleman, D. M.; Dehen, C. J.; Geisler, I. M.; Zemlyanov, D.; Chmielewski, J.; Simpson, G. J.; Wei, A. *Langmuir* **2008**, *24*, 8660−8666. (f) Zhao, Y.; Newton, J. N.; Liu, J.; Wei, A. *Langmuir* **2009**, *25*, 13833−13839.
(58) (a) Beloglazkina, E. K.; Majouga, A. G.; Romashkina, R. B.; Zyk, N. V.; Zefirov, N. S. *Russ. Chem. Rev.* **2012**, *81*, 65−90. (b) Roy, S.; Pericàs, M. A. *Org. Biomol. Chem.* **2009**, *7*, 2669−2677. (c) Wilton-Ely, J. D. E. T. *Dalton Trans.* **2008**, 25−29.
(59) Grabar, K. C.; Freeman, R. G.; Hommer, M. B.; Natan, M. J. *Anal. Chem.* **1995**, *67*, 735−743.
(60) (a) Turkevich, J.; Stevenson, P. C.; Hillier, J. *Discuss. Faraday Soc.* **1951**, *11*, 55−75. (b) Kimling, J.; Mier, M.; Okenve, B.; Kotaidis, V.; Ballot, H.; Plech, A. *J. Phys. Chem.* **2006**, *110*, 15700−15707. (c) Grabar, K. C.; Freeman, R. G.; Hommer, M. B.; Natan, M. J. *Anal. Chem.* **1995**, *67*, 735−743.
(61) Brust, M.; Walker, M.; Bethell, D.; Schiffrin, D. J.; Whyman, R. *J. Chem. Soc., Chem. Commun.* **1994**, 801−802.
(62) Brust, M.; Fink, J.; Bethell, D.; Schiffrin, D. J.; Kiely, C. *J. Chem. Soc., Chem. Commun.* **1995**, 1655−1656.
(63) (a) Dadabhoy, A.; Faulkner, S.; Sammes, P. G. *J. Chem. Soc., Perkin Trans. 2* **2002**, 348−357. (b) Barge, A.; Tei, L.; Upadhyaya, D.; Fedeli, F.; Beltrami, L.; Stefania, R.; Aime, S.; Cravotto, G. *Org. Biomol. Chem.* **2008**, *6*, 1176−1184. (c) Faulkner, S.; Carrie, M.-C.; Pope, S. J. A.; Squire, J.; Beeby, A.; Sammes, P. G. *Dalton Trans.* **2004**, 1405−1409. (d) Grogna, M.; Cloots, R.; Luxen, A.; Jerome, C.; Desreux, J.-F.; Detrembleur, C. *J. Mater. Chem.* **2011**, *21*, 12917−12926.
(64) Following the methods used by (a) Lewis, D. J.; Day, T. M.; MacPherson, J. V.; Pikramenou, Z. *Chem. Commun.* **2006**, 1433−1435. (b) Gopidas, K. R.; Whitesell, J. K.; Fox, M. A. *J. Am. Chem. Soc.* **2003**, *125*, 6491−6502.
(65) Stasiuk, G. J.; Tamang, S.; Imbert, D.; Gateau, C.; Reiss, P.; Fries, P.; Mazzanti, M. *Dalton Trans.* **2013**, *42*, 8197−8200.
(66) Cope, A. C.; Friedrich, E. C. *J. Am. Chem. Soc.* **1968**, *90*, 909−913.
(67) (a) Usón, R.; Laguna, A.; Laguna, M. *Inorg. Synth.* **1990**, *26*, 85−90. (b) Uson, R.; Laguna, A.; Vicente, J. *J. Organomet. Chem.* **1977**, *131*, 471−475.
(68) (a) Matern, E.; Pikies, J.; Fritz, G. *Anorg. Allg. Chem.* **2000**, *626*, 2136−2142. (b) Chatt, J.; Wilkins, R. G. *J. Chem. Soc.* **1956**, 525−529.
(69) Schmidbaur, H.; Wohlleben, A.; Wagner, F.; Orama, O.; Huttner, G. *Chem. Ber.* **1977**, *110*, 1748−1754.
(70) Bailey, J. *J. Inorg. Nucl. Chem.* **1973**, *35*, 1921−1924.
(71) (a) Sullivan, B. P.; Meyer, T. J. *Inorg. Chem.* **1982**, *21*, 1037−1040. (b) Keller, A.; Jasionka, B.; Glowiak, T.; Ershov, A.; Matusiak, R. *Inorg. Chim. Acta* **2003**, *344*, 49−60.
(72) Harris, M. C. J.; Hill, A. F. *Organometallics* **1991**, *10*, 3903−3906.
(73) *SHELXTL PC*; Bruker AXS: Madison, WI. *SHELX-97*: Sheldrick, G. M. *Acta Crystallogr.* **2008**, *A64*, 112−122.